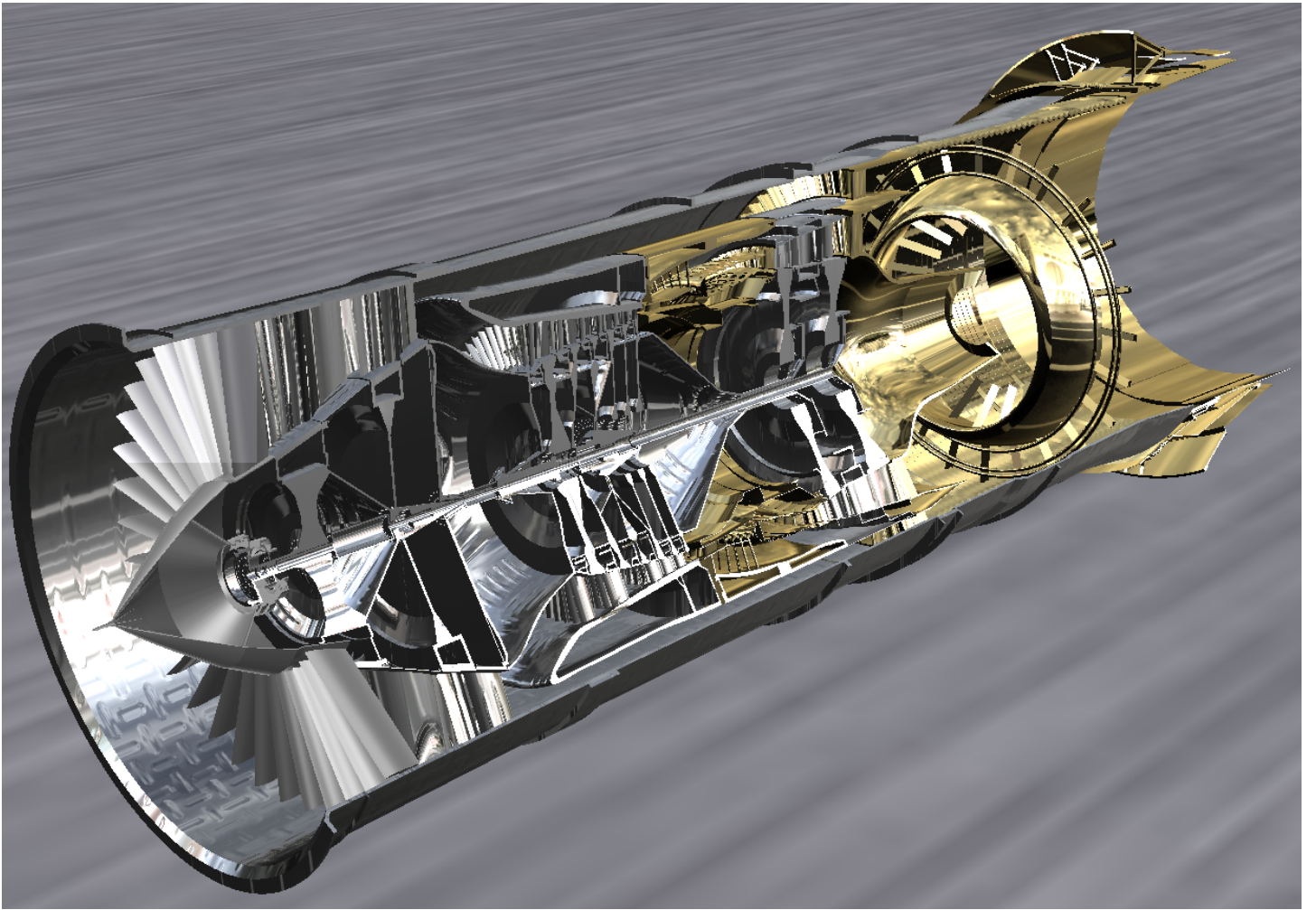


ITU BeEngine for a Next Generation Trainer

AIAA 2015 - 2016
Undergraduate Engine Design Competition
Team ITU BeEngine Proposal



Advisor : Assoc. Prof. Dr. Onur TUNÇER

Team ITU BeEngine

Olcay SARI
Orçun BULAT

ABSTRACT

The aim of this ITU BeEngine Design Project is to design a conceptual new engine to replace GE J-85-5A engine of T-38 supersonic jet trainer with better fuel consumption, performance and weight properties.

New designed BeEngine is capable of providing the required thrust values with an improved fuel consumption values. On the other hand, since the purpose of T-38 is to train pilots for 5th generation fighter aircrafts, better performance properties are included into new engine. With the involvement of latest materials properties, such as TiAl alloys and CMC (Ceramic Matrix Composites), engine weight is decreased significantly for a similar but a little smaller size.

Under the mixed flow low bypass turbofan category, new engine pushes the limits of overall pressure ratio of 16 through 8 compressor stages with a slightly higher bypass ratio of 1.2. Counter rotating 2-spool new engine is aimed to provide optimum values for prepared mission profile for trainer aircrafts while providing extended range of ≈ 1800 nmi. With all ultimate technology limits, each spool is supported by a single stage turbine.

Additionally, BeEngine is quite flexible on the afterburner operations thanks to its higher bypass ratio. Apart from achieving the required afterburner thrust values, it is also possible to increase maximum thrust limit in order to compete with other ultimate supersonic jet trainers in market. Furthermore, with new designed convergent-divergent nozzle with vectoring for allowing extra maneuverability for training purposes.

On last, all the design and dimension selections are done by our team with the programs we have developed.

Special thanks to:
Assoc. Prof. Dr. Onur TUNÇER

May 2016

ITU BeEngine Design Team

Undergraduate Team Engine Design Competition 2015/2016

Request for Proposal:

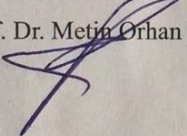
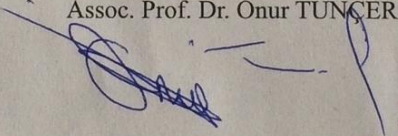
Candidate Engines for a Next Generation Trainer

Title of Design Proposal: ITU BeEngine for a Next Generation Trainer

Name of School: Istanbul Technical University (İstanbul Teknik Üniversitesi)

<u>Designer's Name</u>	<u>AIAA Membership No</u>	<u>Graduation Date</u>	<u>Degree</u>
Olcaey SARI (Team Leader)	675985	March 2016	Aeronautical Eng. (Bachelor)
Team Leader E-mail address: olcaey.sari@gmail.com			
Orçun BULAT (Team Member)	609386	July 2016	Aeronautical Eng. (Bachelor)

AIAA Foundation will act as the administrator for this competition.

<u>Signature of Faculty Advisor</u>	<u>Signature of Project Advisor</u>	<u>Date</u>
Prof. Dr. Metin Orhan KAYA 	Assoc. Prof. Dr. Onur TUNÇER 	26.04.2016



Team Leader: Olcaey SARI



Team Member: Orçun BULAT

The design process was followed under UCK 474E – Aircraft Engine Design lecture of Istanbul Technical University that was instructed by Assoc. Prof. Dr. Onur TUNÇER on the fall term of 2015/2016. The design is completed by end of the lecture on February 2016 and presented in order to complete the course. Afterwards, additional analyses and technical drawings (2D & 3D) have been made prepared. By May, project is finalized and submitted to AIAA Undergraduate Competition.

<i>TABLES</i>	<i>Page</i>
<i>ABSTRACT</i>	<i>i</i>
<i>ACRONYMS</i>	<i>iv</i>
<i>LIST OF TABLES</i>	<i>v</i>
<i>LIST OF FIGURES</i>	<i>vi</i>
<i>1. INTRODUCTION</i>	<i>1</i>
1.1. Aircraft Specifications	<i>1</i>
1.2. Performance and Engine Requirements	<i>1</i>
1.3. Baseline Engine Model Characteristics	<i>2</i>
1.4. Market Evaluation & Technological Stand Point	<i>2</i>
1.4.1 Advanced Jet Trainers	<i>2</i>
1.4.2 5 th Generation Jet Fighters	<i>2</i>
<i>2. CONSTRAINT & MISSION ANALYSIS</i>	<i>4</i>
2.1. Performance Requirements Evaluation	<i>4</i>
2.2. Constraint Analysis Diagram and New Engine Design Value	<i>4</i>
2.3. Mission Analysis Evaluation	<i>5</i>
<i>3. PARAMETRIC CYCLE & PERFORMANCE ANALYSES</i>	<i>7</i>
3.1. Engine Design Variables	<i>8</i>
3.2. Parametric Cycle Analysis of Mixed Flow Turbofan	<i>8</i>
3.3. Sensitivity Analysis	<i>13</i>
3.4. Performance Analysis Evaluation	<i>13</i>
3.5. In-Depth Analysis for Engine Design	<i>14</i>
3.5.1. Mission Fuel Burn Analysis	<i>14</i>
3.5.2. Cruise TSFC Analysis	<i>16</i>
3.5.3. Engine Weight Analysis	<i>19</i>
<i>4. COMPRESSOR DESIGN</i>	<i>20</i>
4.1. Fan Design & Calculations	<i>21</i>
4.2. High Pressure Compressor Design & Calculations	<i>23</i>
4.3. Compressor Blade Geometry & Airfoil Selection	<i>26</i>
4.4. Blade Number Measurement	<i>28</i>
4.5. Blade Stress Evaluation and Material Selection	<i>29</i>
<i>5. TURBINE DESIGN</i>	<i>29</i>
5.1. High Pressure Turbine (HPT) Design	<i>30</i>
5.2. HPT Structural Analysis	<i>32</i>
5.3. Low Pressure Turbine (LPT) Design	<i>34</i>
5.4. Turbine Blade Geometry	<i>36</i>
5.5. LPT Structural Analysis	<i>36</i>
<i>6. INLET DESIGN</i>	<i>37</i>
<i>7. COMBUSTION SYSTEMS DESIGN</i>	<i>39</i>
7.1. Main Burner	<i>39</i>
7.2. After-Burner	<i>40</i>
<i>8. NOZZLE DESIGN</i>	<i>42</i>
<i>9. CONCLUSION</i>	<i>44</i>
<i>REFERENCES</i>	<i>I</i>
<i>APPENDIX A - Performance Analysis – Iterative Solution Method Scheme</i>	<i>II</i>

ACRONYMS

AAF	: Air-to-air Fighter
AIAA	: The American Institute of Aeronautics and Astronautics
BPR	: By-Pass Ratio
C-D	: Convergent - Divergent
CFD	: Computational Fluid Dynamics
EF	: Endurance Factor
FPR	: Fan Pressure Ratio
GE	: General Electric
HPC	: High Pressure Compressor
HPT	: High Pressure Turbine
IGV	: Inlet Guide Vane
NACA	: National Advisory Committee for Aeronautics
NASA	: National Aeronautics and Space Administration
NPR	: Nozzle Pressure Ratio
OPR	: Overall Pressure Ratio
LPC	: Low Pressure Compressor
LPT	: Low Pressure Turbine
RF	: Range Factor
RFP	: Request for Proposal
RPM	: Revolutions per Minute
SLS	: Sea Level Static
TIT	: Turbine Inlet Temperature
TL	: Thrust Loading
TO	: Take-Off
TR	: Throttle Ratio
TSFC	: Thrust Specific Fuel Consumption
WL	: Wing Loading

LIST OF TABLES**Page**

Table 1.1 : Some General Characteristics of the Next Generation Trainer.....	1
Table 1.2 : Performance Requirements for New Engine.....	1
Table 1.3 : In-Flight Thrust Requirements.....	1
Table 1.4 : Baseline Engine: Basic Data, Overall Geometry and Performance.....	2
Table 1.5 : Supersonic Jet Trainer Aircrafts.....	3
Table 1.6 : 5 th Generation Jet Fighter Aircrafts.....	3
Table 2.1 : Performance Requirements for Constraint Analysis.....	4
Table 2.2 : Primary Mission Profile for Advanced Jet Trainer & Weight Fraction....	6
Table 2.3 : Aircraft Specifications.....	7
Table 3.1 : Engine Design Variables.....	8
Table 3.2 : Primary Design Selection Values.....	12
Table 3.3 : Parametric Cycle Analysis (at SLS) Summary in Wet Condition.....	13
Table 3.4 : Sensitivity Analysis.....	13
Table 3.5 : Performance Analysis Results.....	14
Table 3.6 : Mission Fuel Burn – In-depth Analysis I.....	15
Table 3.7 : Mission Fuel Burn – In-depth Analysis II.....	15
Table 3.8 : Mission Fuel Burn – In-depth Analysis III.....	16
Table 3.9 : Weight Estimation Comparison – 5th Generation Fighters.....	19
Table 3.10 : Weight Estimation Comparison – Jet Trainers.....	19
Table 3.11 : New Engine Design Options Weight Estimation Comparison.....	20
Table 3.12 : BeEngine vs J85-5A.....	20
Table 4.1 : Fan Design Parameters & Values.....	21
Table 4.2 : Fan Design Output Values – Fan Stages 1 & 2.....	22
Table 4.3 : High Pressure Compressor Design Parameters & Values.....	23
Table 4.4 : High Pressure Compressor Output Values – Stages 1/2.....	24
Table 4.5 : High Pressure Compressor Output Values – Stages 2/2.....	25
Table 4.6 : Fan Repeating Design Stages Blade Angles (degree).....	26
Table 4.7 : Fan Stages Blade Dimensions.....	27
Table 4.8 : HPC Repeating Design Stages Blade Angles (degree).....	27
Table 4.9 : HPC Stages Blade Dimensions.....	27
Table 4.10 : Design and Assumption Values for Engine Rotor & Stator Blades.....	28
Table 4.11 : Blade Numbers of Each Compressor Stage.....	28
Table 4.12 : Fan/LPC Blade Stress Calculations.....	29
Table 4.13 : HPC Blade Stress Calculations.....	29
Table 5.1 : High Pressure Turbine Design Point Parameters.....	30
Table 5.2 : HPT Results – I.....	31
Table 5.3 : HPT Results – II.....	31
Table 5.4 : HPT Stage Turbine Blade Measurements.....	33
Table 5.5 : Low Pressure Turbine Design Point Parameters.....	34
Table 5.6 : LPT Results – I.....	35
Table 5.7 : LPT Results – II.....	35
Table 5.8 : HPT Stage Blade Geometries.....	36
Table 5.9 : LPT Stage Blade Geometries.....	36
Table 5.10 : LPT Stage Turbine Blade Measurements.....	37
Table 6.1 : Ramp Angles & Inlet Output.....	38
Table 6.2 : Inlet Diffuser Duct Data.....	38
Table 7.1 : Main Burner Stations & Dimensions.....	39
Table 7.2 : Air Partitions at $T_g = 1950\text{K}$ (3510°R) & $\epsilon_{pZ} = 0.8$	40
Table 7.3 : Main Burner Zones Geometry.....	40

Table 7.4 : Main Burner Geometry	40
Table 7.5 : Flow Areas before After-Burner Section	41
Table 7.6 : Mixer & Diffuser Dimensions	41
Table 7.7 : Combustion Parameters	42
Table 8.1 : Nozzle Design Input Values.....	43
Table 8.2 : Nozzle Design Output Values	43
Table 9.1 : J85-5A & New Engine Comparison Summary	44
Table 9.2 : New Engine Component vs. Material Summary.....	44

LIST OF FIGURES

	<u>Page</u>
Figure 2.1 : Constraint Diagram - Wing Loading (lbf/ft ²) vs. Thrust Loading.....	5
Figure 2.2 : Primary Mission Profile by Phases.....	5
Figure 2.3 : Weight & Fuel Usage for Primary Mission Profile	7
Figure 3.1 : Parametric Cycle Analysis (dry) – BPR vs OPR @SLS	9
Figure 3.2 : Parametric Cycle Analysis (dry) – FPR vs OPR (BPR = 1.2).....	9
Figure 3.3 : Parametric Cycle Analysis (dry) – FPR vs BPR (OPR = 16).....	10
Figure 3.4 : Parametric Cycle Analysis (dry) – BPR vs TIT (OPR = 16).....	10
Figure 3.5 : Parametric Cycle Analysis (dry) – OPR vs TIT (BPR = 1.2).....	11
Figure 3.6 : Parametric Cycle Analysis (wet) – OPR & BPR (T ₁₇ = 2000 K)	11
Figure 3.7 : Parametric Cycle Analysis (wet) – OPR & T ₁₇ (BPR = 1.2)	12
Figure 3.8 : Performance Analysis – Cruise, OPR & FPR	17
Figure 3.9 : Performance Analysis – Cruise, BPR & FPR.....	17
Figure 3.10 : Performance Analysis – Cruise, OPR & TiT (BPR = 1.2)	18
Figure 3.11 : Performance Analysis – Cruise, BPR & TiT (OPR = 16)	18
Figure 3.12 : Estimated Engine Weight Variation (Mass Flow = 50 lbf/s).....	20
Figure 4.1 : Fan/LPC 1 st Stage Velocity Triangles (mean).....	26
Figure 4.2 : HPC 1 st Stage Velocity Triangles (mean).....	26
Figure 5.1 : HPT Stage Velocity Triangles (mean).....	32
Figure 5.2 : AN ² as a Function of Specific Strength and Taper Ratio	34
Figure 5.3 : Comparison of 100h tensile creep rate	34
Figure 5.4 : LPT Stage Velocity Triangle (mean).....	35
Figure 6.1 : Inlet Geometry	39
Figure 7.1 : Swirler Design & Layout.....	40
Figure 7.2 : Mixer & Diffuser Layout.....	41
Figure 7.3 : Flameholders Layout	42
Figure 8.1 : New Convergent – Divergent Nozzle Geometry.....	44
Figure 9.1 : BeEngine 2D Preliminary Technical Draftings.....	46
Figure 9.2 : BeEngine 3D Technical Drawing	47

General characteristics	
Wing area	170 ft ²
Max. take-off weight	12 000 lbm
Takeoff-Thrust (dry)	2750 lbf
Design Afterburning Thrust (wet)	4500 lbf
Performance	
Maximum speed	1.4 Mach
Cruise speed	0.85 Mach
Mission Fuel Burn	2871 lbf
Cruise TSFC	0.81 (lbm/h/(lbf))
Takeoff TSFC	0.66 (lbm/h/(lbf))
Engine Weight	424.2 lbm
Fan Diameter	18 in
Summary Data	
Design MN	0 (SLS)
Design Altitude	0 (SLS)
Design Fan Mass Flow	50 lbm/s
Design Gross Thrust	4600 lbf
Design Bypass Ratio	1.2
Design Net Thrust (dry)	2750 lbf
Design Afterburning Net Thrust	4500 lbf
Design TSFC (lbm/h/(lbf))	0.66 (dry) & 1.76 (wet)
Design Overall Pressure Ratio	16
Design T4.1	1480 K - 2664 °R
Design Engine Pressure Ratio	2.51 (dry) & 2.41 (wet) @SLS
Design Fan / LPC Pressure Ratio	2.3
Design Chargeable Cooling Flow (% @25)	1.5 % - 0.341 lbm/s
Design Non-Chargeable Cooling Flow (% @25)	1.5 % - 0.341 lbm/s
Design Adiabatic Efficiency for Each Turbine	HPT: 90.2% - LPT: 91.7%
Design Polytropic Efficiency for Each Compressor	Fan: 89% - HPC: 90%
Design HP/LP Shaft RPM	HP: ≈ 25783 - LP: ≈ 17562
Additional Information	
Design HP/LP Shaft Off-take Power	HP: 105.03 KW - LP: 0
Design Customer Bleed Flow	0.2273 lbm/s (1%)

* Rest of the information that is not added into the RFP tables can be found inside the report.

1. INTRODUCTION

AIAA Undergraduate Team Engine Design Competition 2015/16 project RFP [U1], “Candidate Engines for a Next Generation Trainer” is about designing a new turbofan engine that is solicited for an advanced trainer capable of replacing the T-38, which is expected to enter service around 2025. The new aircraft must be capable of emulating 5th generation fighter aircraft and training 5th generation pilots.

Main challenges are increased Mach number capabilities with improved fuel consumption and performance properties while decreasing the engine weight. Besides, range should be increased with the new engine thanks to its improved cruise TSFC.

1.1. Aircraft Specifications

The trainer jet under consideration should allow for simulation of advanced 5th generation fighters for pilot training. It has a plan form which is similar in wing and tail shape and arrangement to the T38A trainer. It will dash at Mach 1.3 over land and can also cruise at Mach 0.85, offering a lower cost-per-mile than the T-38.

Table 1.1 : Some General Characteristics of the Next Generation Trainer

<i>Aircraft General Characteristics</i>	
Crew	2
Length	46.0 ft
Wing Span	25.25 ft
Height	13.8 ft
Wing Area	170 ft ²
Max. Take-Off Weight	12 000 lbm
Power Plant	2 x low bypass ratio turbofans; 4000 lbf each @SLS

While engine may exceed the thrust requirements at any given point, this may lead to excess fuel consumption. Fan diameter should be limited to 20” for compatibility with aircraft.

1.2. Performance and Engine Requirements

Table 1.2 : Performance Requirements for New Engine

<i>Performance</i>	
Max. Speed	Mach 1.3 at 40 000 ft (Afterburning)
Cruise Speed	Mach 0.85 at 35 000 ft (Cruise, no Afterburning)
Range	At Mach 0.85; 1500 nmi
Loiter	Mach 0.5 @ 15000 feet for 30 mins
Service Ceiling	51 000 ft (16 000 m)

Table 1.3 : In-Flight Thrust Requirements

<i>General Thrust Requirements (Total for 2 engines)</i>		
Takeoff	Sea Level Static + 27F Std. Day	8 000 lbf
Cruise	Mach 0.85, 35 000 ft	1 270 lbf
Supersonic Flight	Mach 1.3, 40 000 ft	3 000 lbf
Loiter	Mach 0.5, 15 000 ft	2 460 lbf

1.3. Baseline Engine Model Characteristics

Table 1.4 : Baseline Engine: Basic Data, Overall Geometry and Performance

<i>Design Features of the Baseline Engine</i>	
Engine type	Axial, turbojet
Number of compressor stages	9
Number of HP turbines stages	2
Combustor type	Annular
Maximum net thrust at sea level (wet)	3,850 lbf
Specific Fuel Consumption at max. power (wet)	2.2 lbm/hr/lbf
Overall pressure ratio at max. power	6.7
Max. envelope diameter	17.7 inches
Max. envelope length	51.1 inches
Dry weight less tail-pipe	421 lbm

1.4. Market Evaluation & Technological Stand Point

At the beginning of the design phase, it is very important to be aware of the market situation of the industry to be working upon. For this reason, a wide range of research has been made for gathering information of jet trainer aircrafts and 5th generation fighters. Furthermore, their properties are very important for the new engine and its design due to the purpose of new trainer aircraft.

1.4.1 Advanced Jet Trainers

With the creation of 4th and 5th generation fighter aircrafts which are capable of high maneuvers and own enhanced avionic systems, new type of trainers – Advanced Jet Trainers have been developed to train latest generation pilots. While providing the opportunity of simulating latest fighter aircrafts missions and properties, the unit price and operational costs of the trainers should be as low as possible to fulfill their purpose, which is aimed for the next generation of T-38.

Moreover, NASA has been using T-38 for training astronauts for high-g climbing to simulate launch condition. [U2]

1.4.2 5th Generation Jet Fighters

The latest generation of jet fighters – 5th encompasses the most advanced fighter aircrafts. Even though the exact characteristics of 5th generation still hasn't been absolutely clear yet, some of the aimed properties of this generation [1] are:

- All-aspect stealth property,
- High maneuverability,
- Short field capabilities,
- Advanced avionic features,
- High-performance airframes.

For now, there has been only few type of aircrafts are considered to be named under 5th generation, which are going to be evaluated and taken into consideration while working on the new trainer engine design.

On tables 1.5 and 1.6, information about similar aircrafts and their engines are gathered. [2, U3, U4, U5, U6, U7, U8]

Table 1.5 : Supersonic Jet Trainer Aircrafts

	T-38 Talon		T-50 GE		Hongdu L-15		JL-9		F-5B	
Engine Type	J85-GE-5A [2]		GE F404 [2]		AI-222-25F [U3]		Tumansky R-13 [2]		J85-GE-13 [2]	
Properties	DRY	WET	DRY	WET	DRY	WET	DRY	WET	DRY	WET
Thrust (lbf)	2680	3850	11000	17700	5550	9260	8970	14320	2720	4080
TSFC (1/h)	1.03	2.20	0.81	1.74	0.66	1.9	0.91	2.09	1.26	2.22
Airflow (lbm/s)	44.1		146		49.7		145.5		44	
OPR	6.7		26		15.43		8.9		6.5	
Bypass Ratio	6.7		0.34		1.19		N/A		-	
Compressors	9		3F, 0L, 7H		2L, 8H		3L, 5H		9	
Turbines	2		1H, 1L		1H, 1L		1H, 1L		2	
Diameter (in)	22		35		24.56		43.1		22	
Length (in)	108.1		154		123.543		181.3		108.9	
Weight (lbm)	584		2282		1190		2656		597	

Table 1.6 : 5th Generation Jet Fighter Aircrafts

	F-22 Raptor		F-35		PAK FA T-50		Mitsubishi X-2 Shingun		Chengdu J-20	
Engine Type	P&W F119-PW-100 [U4, 3]		P&W F135 [U5,U6]		AL-41F1 (117S) [U7]		IHI XF-5 [U8]		AL-31F [U9]	
Properties	DRY	WET	DRY	WET	DRY	DRY	DRY	WET	DRY	WET
Thrust (lbf)	26000	>35000	28000	43000	N/A	N/A	17850	27560	17850	27560
TSFC (1/h)	0.8	2.17	0.7	1.95	N/A	N/A	0.657	N/A	0.657	N/A
Airflow (lbm/s)	270		307.8		N/A		100		243	
OPR	26.8		28		N/A		26		23	
Bypass Ratio	0.45		0.57		Variable		0.39		0.57	
Compressors	3F, 0L, 6H		3F, 0L, 6H		4L, 9H		3F, 0L, 6H		9H	
Turbines	1H, 1L		1H, 1L		N/A		1H, 1L		1H, 2L	
Diameter (in)	48		51		N/A		20		48	
Length (in)	203.15		220		N/A		100		195	
Weight (lbm)	3900		3750		3130		1420		3373	

2. CONSTRAINT & MISSION ANALYSIS

The initial phase of engine design starts with the evaluation of constraint analysis for its aircraft. Afterwards, a design point for new engine has been selected and a potential mission analysis has examined.

2.1. Performance Requirements Evaluation

From the given RFP, the lack of expected mission profile and required behaviors of the aircraft caused a deep research on potential jet trainer aircraft mission profiles and behaviors. For this purpose, the supersonic jet trainer aircrafts and 5th generation aircrafts are considered.

Table 2.1 : Performance Requirements for Constraint Analysis

Take-Off	2000ft PA, $T(^{\circ}\text{F})=100$, $S_{\text{TO}}=S_{\text{G}}+S_{\text{R}} \leq 3000\text{ft}$, $k_{\text{TO}}=1.2$, $\mu_{\text{TO}}=0.05$, $t_{\text{R}}(\text{s})=3$
Cruise	$h(\text{ft})=35000$, $M=0.85$
Max Mach	$h(\text{ft})=40000$, $M=1.3$
Loiter	$h(\text{ft})=15000$, $M=0.5$, $n=1$, $t_{\text{loiter}}(h)=0.5$
Service Ceiling	$h(\text{ft})=51000$, Max Power
Landing	2000ftPA, $T(^{\circ}\text{F}) = 100$, $S_{\text{FR}}+S_{\text{BR}} \leq 2700\text{ft}$, $k_{\text{TD}}=1.15$, $\mu_{\text{B}}=0.18$, $t_{\text{FR}}(\text{s})=3$

All taken values above have been considered with different causes:

- Take-off distance of 3000 ft and landing distance of 2700 ft values are taken from T-38 Flight Manual [5].
- Average airport runway altitude is considered as 2000 ft therefore take-off altitude is selected 2000 ft. Besides, any altitude right above the sea level effect the pressure altitude by 2 or 3 times.
- In T-38 Flight Manual [5], stall speed is given as 0.1918 Mach, corresponding M_{TO} is estimated as 0.23.
- Throttle ratio is taken as 1.08.

Additionally, an extra calculation has been made to analyse high maneuverability of new jet trainer because of the properties of 5th generation fighters.

2.2. Constraint Analysis Diagram and New Engine Design Value

The values of K_1 , K_2 , C_{D0} and C_{DR} , technological limits and general aircraft values are taken into consideration as future jet aircraft when making calculations [4]. Lift coefficient (C_L) value for T-38 is considered as 1.2 in the calculations [5].

Maximum and Military Power equations [4] above with the reference baseline engine are used to create constraint diagram in order to select for the new design engine values.

In Constraint Diagram figure, (x) points show the trainer aircrafts, (o) points show the fighters and red points show the 5th generation of aircrafts (either developed as 5th generation or modernized to 5th generation). Thanks to the distribution of all points and initial evaluation, a design point for the new engine is estimated.

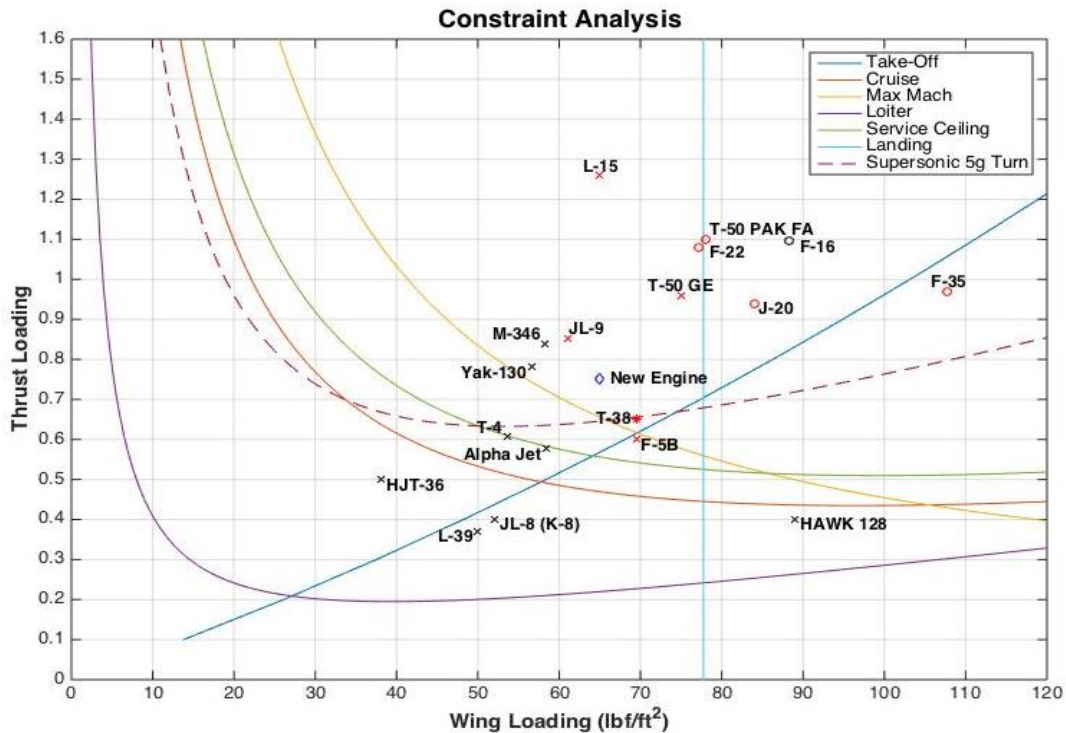


Figure 2.1 : Constraint Diagram - Wing Loading (lb/ft²) vs. Thrust Loading

“Supersonic 5g Turn” constraint boundary line is calculated and added to graph in order to check the maneuverability of new aircraft / engine.

For the thesis, after the evaluation of the similar advanced jet trainers, design values are selected accordingly:

- Thrust Loading = 0.75
- Wing Loading = 65 lb/ft²

Selection includes the assumption of engine weight reduction and better fuel efficiency.

2.3. Mission Analysis Evaluation

Before going through the mission analysis, a mission profile for T-38 aircraft needs to be developed. For this purpose, examples from other mission profiles of jet trainers and 5th generation fighters are researched and evaluated. [U9, U10, 4]

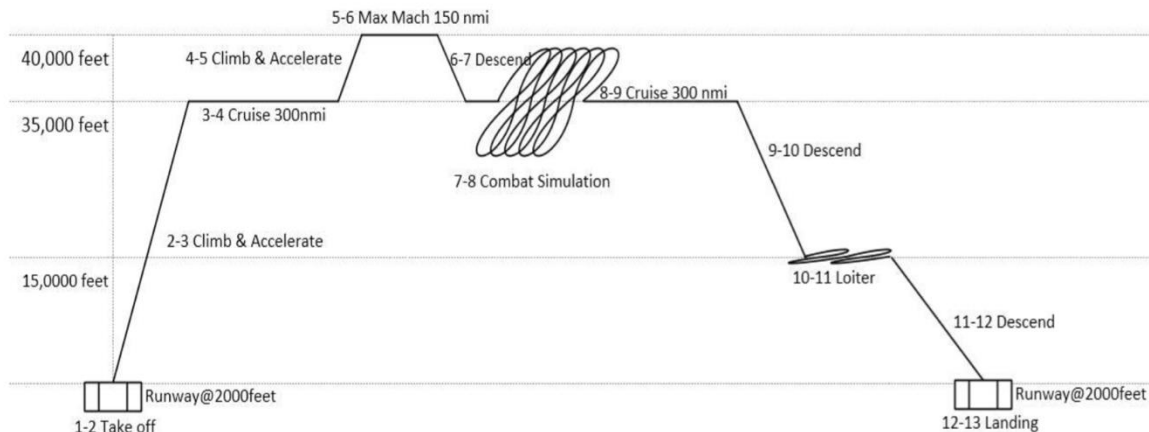


Figure 2.2 : Primary Mission Profile by Phases

Table 2.2 : Primary Mission Profile for Advanced Jet Trainer & Weight Fraction

Phase	Mission Segments	Beta	Wf / Wi	Fuel Used (lbf)
1 - 2	Takeoff h = 2 000 ft , $\Delta s_{TO} \leq 3\ 000$ ft, 100°F	0.9823	0.9823	195.62
2 - 3	Climb & Accelerate M: 0.23 \rightarrow 0.85 , h: 2 000 ft \rightarrow 40 000 ft	0.9531	0.9703	322.60
3 - 4	Cruise M = 0.85 , h = 35,000ft , $\Delta s = 300$ nmi	0.9171	0.9623	397.28
4 - 5	Climb & Accelerate M: 0.85 \rightarrow 1.3 , h: 35 000 ft \rightarrow 40 000 ft	0.9016	0.9830	171.79
5 - 6	Max. Mach M = 1.3 , h = 40 000 ft , $\Delta s = 150$ nmi	0.8570	0.9505	493.06
6 - 7	Descend h: 40 000 ft \rightarrow 35 000 ft	0.8570	1	0
7 - 8	Combat Simulation	0.8141	0.95	473.48
8 - 9	Cruise M = 0.85 , h = 35 000 ft , $\Delta s = 300$ nmi	0.7823	0.9609	351.99
9 - 10	Descend h: 35 000 ft \rightarrow 15 000 ft	0.7842	1	0
10 - 11	Loiter M = 0.5 , h = 15 000 ft , $\Delta t = 30$ mins	0.7438	0.9509	424.76
11 - 12	Descend & Land h = 2 000 ft , $\Delta s_L \leq 2\ 700$ ft, 100°F	0.7401	0.995	41.10
	Total	0.74	-	2871.89

The weight fraction on each profile segment in the mission profile and final situation has been found as the Table 2.2. For the estimated amount of used fuel, W_{TO} is taken as 11,050 lbf.

Engine requirements are considered together with 5th generation fighter aircraft mission and other examples in the mission profile. Besides, “Combat Simulation” is added to the mission, however it is not specified in details to provide flexibility to the training content. Possible actions under combat simulation might be:

- 1.2M 5g turn at 15 000 ft
- 0.8M 5g 2-turns at 15 000 ft
- Acceleration from 0.7M to 1.2M at 15 000 ft

Before 6ptimized6 this chapter, the range of aircraft is compared with the result from the Range Factor (RF) equation [4]. The maximum range of 1500nmi with loiter results in a final weight fraction of 0.745, which is very close to 0.74. Therefore, values and calculations seem to be logical for constraint and mission analysis for the desired range.

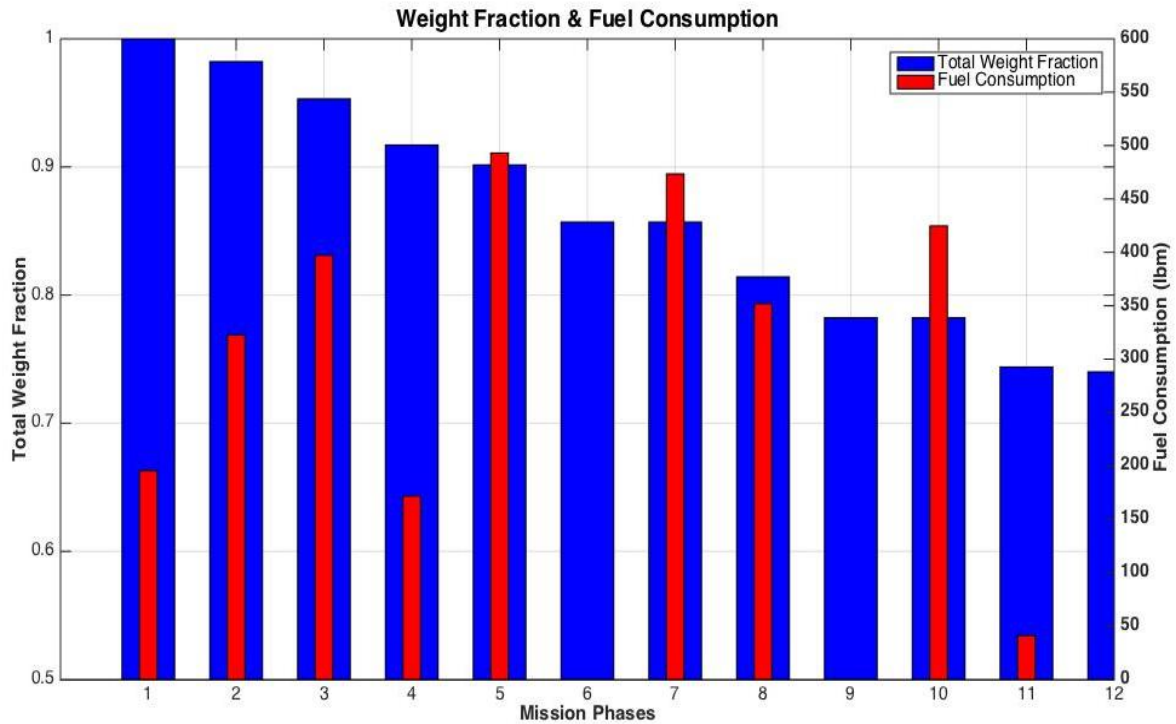


Figure 2.3 : Weight & Fuel Usage for Primary Mission Profile

Table 2.3 : Aircraft Specifications

Aircraft Specifications	
Take-Off Weight	11050 lbf
Thrust Sea Level	8000 lbf
Wing Area	170 ft ²
Payload	1379 lbf
Empty Weight	6800 lbf
Fuel Weight	2871 lbf
Thrust Loading	0.75 lbf/ft ²
Wing Loading	65

3. PARAMETRIC CYCLE & PERFORMANCE ANALYSES

Parametric cycle analysis is a dimensionless design to show the connection between major design parameters and how they effect the the performance of our engine. Thanks to the variation of each design parameter and their combination, we would be able to perform different working requirements of the engine.

On this part, main parameters and specifications are going to be determined. Afterwards, design parameters will help on defining the performance and constraints of the engine for both on design and off design conditions.

Sea Level Static (SLS) condition is selected for parametric cycle – on design analysis. Other conditions of cruise, supersonic flight and loiter conditions will be evaluated on off-design performance analysis.

3.1. Engine Design Variables

Determination of design parameters is crucial for aircraft engine design, especially to reach out to a high quality result. In order to be successful on the design, variable sources from the history of aviation is going to be used.

Pareto Principle states that the 20% of the main sources / inputs are directly effective on the 80% of the results / outcomes. Therefore, the main design parameters need to be paid most attention. The 6 most important parameters are used in order to make parametric cycle analysis.

Table 3.1 : Engine Design Variables

Aircraft system parameters	$\beta, P_{TOL}, P_{TOL}, \varepsilon_1, \varepsilon_2$
Design limitations	T_{t4-max}, T_{t7-max}
Fuel Heating Value	h_{fuel}
Polytropic efficiencies	$\eta_{burner}, \eta_{AB}, \eta_{mech}, \eta_{mL}, \eta_{mH}$
Component performances	π_{fd}, π_M
Total pressure losses	$\pi_{intake}, \pi_{Mmax}, \pi_{burner}, \pi_{AfterBurner}, \pi_{JetPipe}, \pi_{nozzle}$
Design Choices	$\dot{m}, \pi_t, \pi_{cL}, \pi_{cH}, \alpha, T_{t4}, T_{t7}, M_{mix}$

The historical data and trends together with latest technological capabilities on the on-design cycle analysis are considered from Mattingly [4] and Farokhi [6].

On parametric cycle analysis, design conditions are:

- $h = 0$ ft where $P_0 = 14.7$ psia and $T_0 = 545$ R (SLS +27F Std. Day conditions)
- $M_0 = 0$

The the percentage of internal cooling values are considered as following due to the reliability for the health of engine:

$$\varepsilon_1 = 0.015 \quad \& \quad \varepsilon_2 = 0.015 \quad (3\% \text{ of air in total})$$

3.2. Parametric Cycle Analysis of Mixed Flow Turbofan

The major graphic is prepared with the variation of bypass and operational pressure ratios. For this cycle analysis, TIT temperature is considered as 1500K. Besides, nozzle is choked and perfectly extended in order to obtain the highest thrust values for each α and π_c design conditions calorifically perfect gas assumption.

In order to make design parameters selected, few other graphical calculations and comparisons are going to be made on parametric cycle analysis. In order to obtain carpet plots of parametric cycle analysis, other design parameters are considered as constant on variable values.

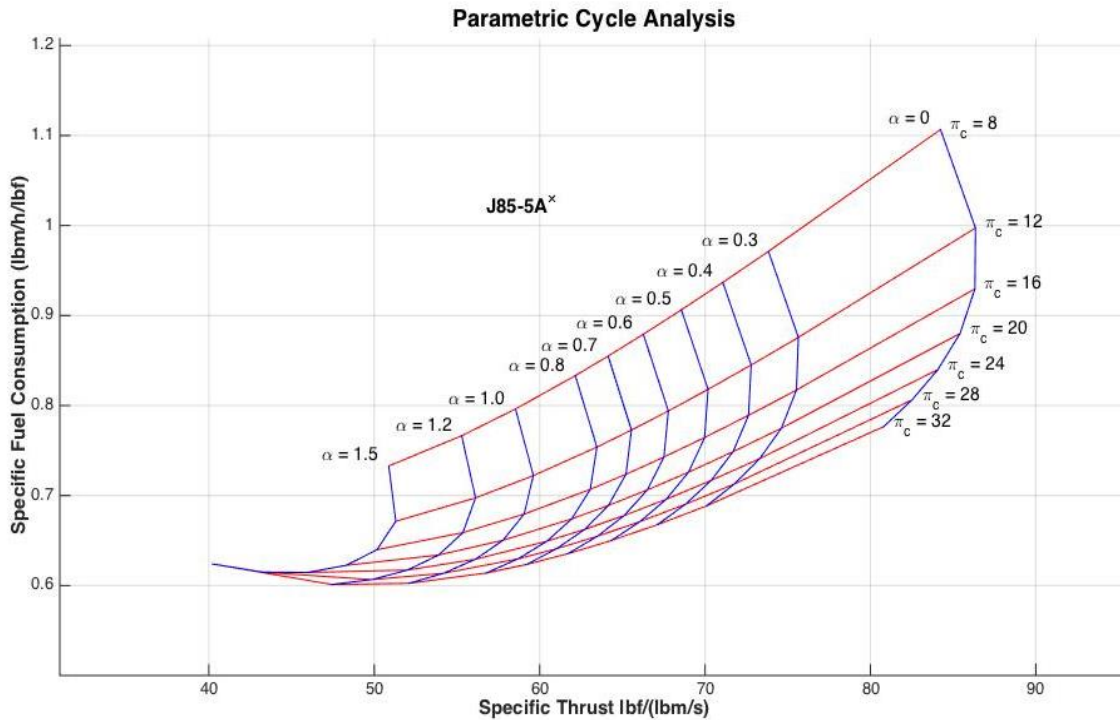


Figure 3.1 : Parametric Cycle Analysis (dry) – BPR vs OPR variation at SLS condition

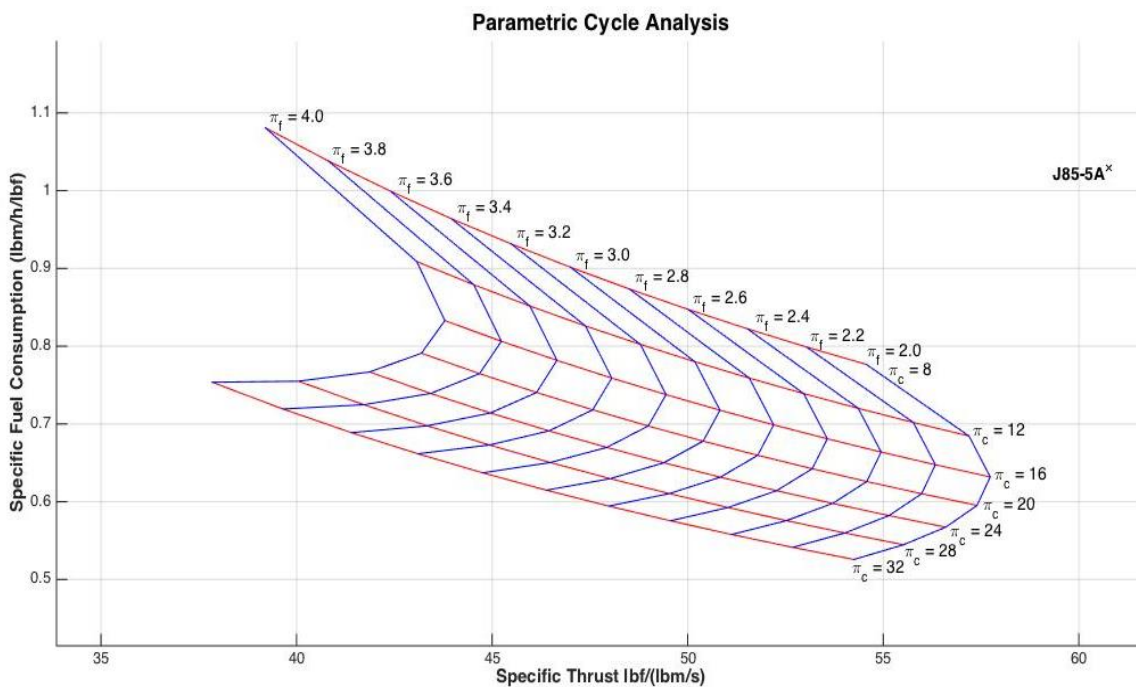


Figure 3.2 : Parametric Cycle Analysis (dry) – FPR vs OPR variation (BPR = 1.2)

By-pass ratio above 1.0 provides better fuel consumption efficiencies and difference than lower by-pass ratios. However, on the other hand, increasing by-pass ratio decreases specific thrust value for the engine significantly. Therefore, it is important to select a by-pass ratio that enables the thrust requirements for both on-design and off-design conditions.

For a certain overall pressure ratio, the fan pressure ratio and bypass ratio variation is shown in Figure 3.3. For a BPR above 1.0, lower FPR is desired in order to increase the specific thrust value while decreasing the SFC.

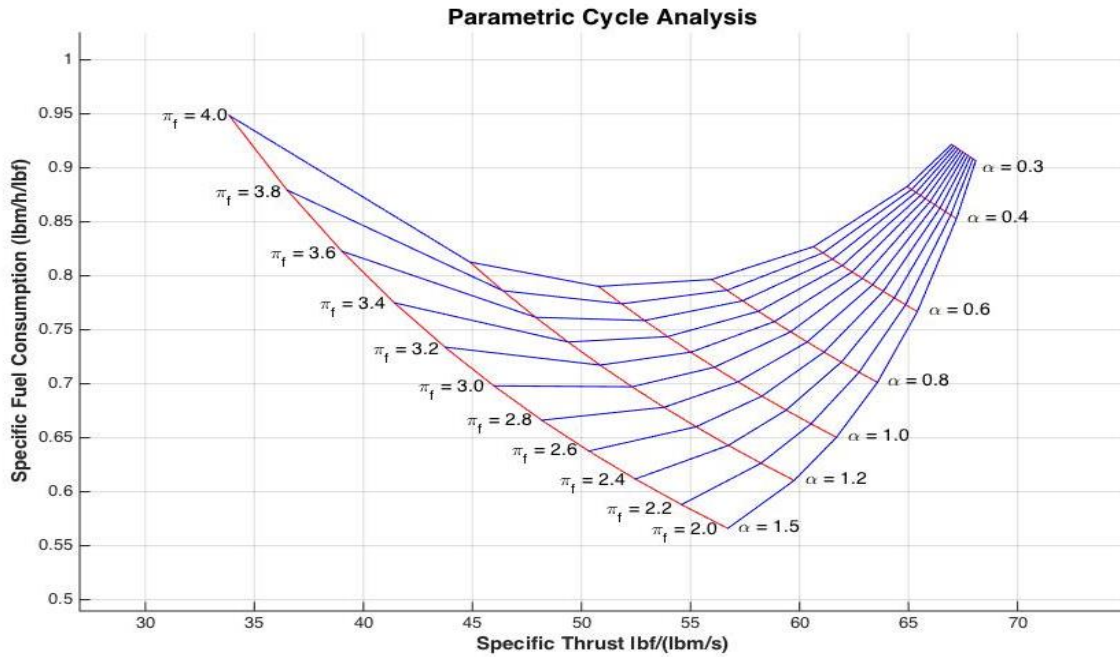


Figure 3.3 : Parametric Cycle Analysis (dry) – FPR vs BPR variation (OPR = 16)

Turbine Inlet Temperature ($TIT - T_{t4}$) has direct relation with SFC and specific thrust values. The baseline engine has 1120 K TIT, however with the consideration of selection new OPR parameter around 16 makes TIT potentially higher than the baseline engine.

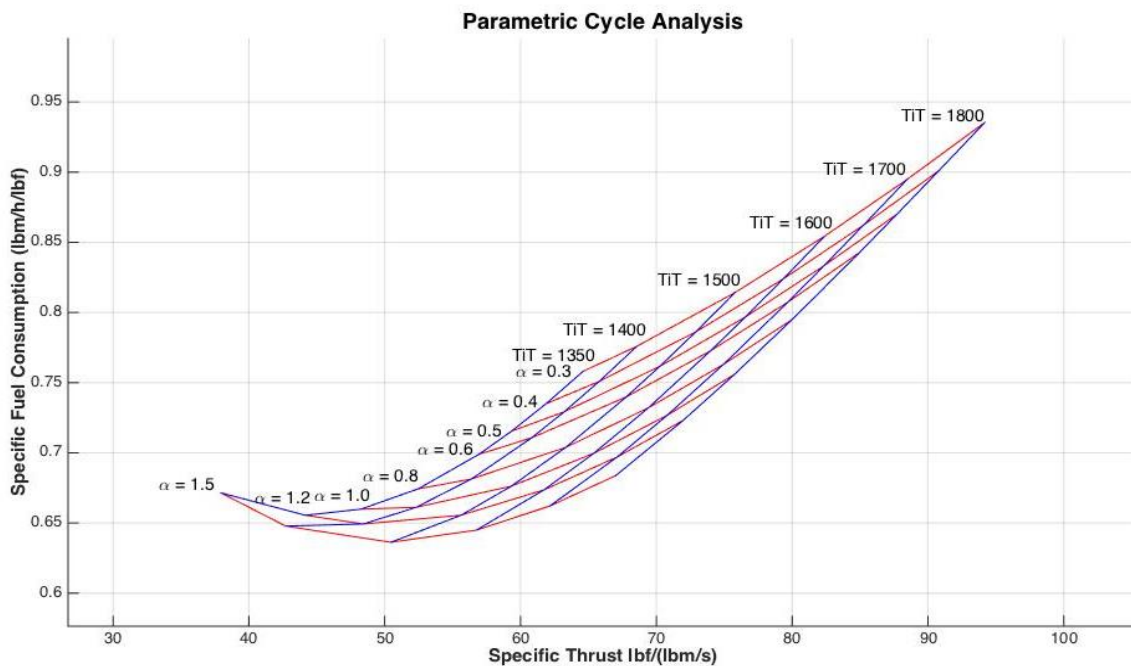


Figure 3.4 : Parametric Cycle Analysis (dry) – BPR vs TIT variation (OPR = 16)

The increasing TIT corresponds to a minimum SFC value for each OPR. As shown in figure 3.4, BPR values of 1.0, 1.2 and 1.5 has minimum SFC for certain TIT values.

When BPR is lower than 1.0, the specific thrust value higher than higher BPR engines, as well as SFC. For the cruise case, according to the required thrust and baseline thrust, potential selection of BPR higher than 1.0 seems a feasible design option. However, before this preference, further investigation on wet condition and TIT is needed.

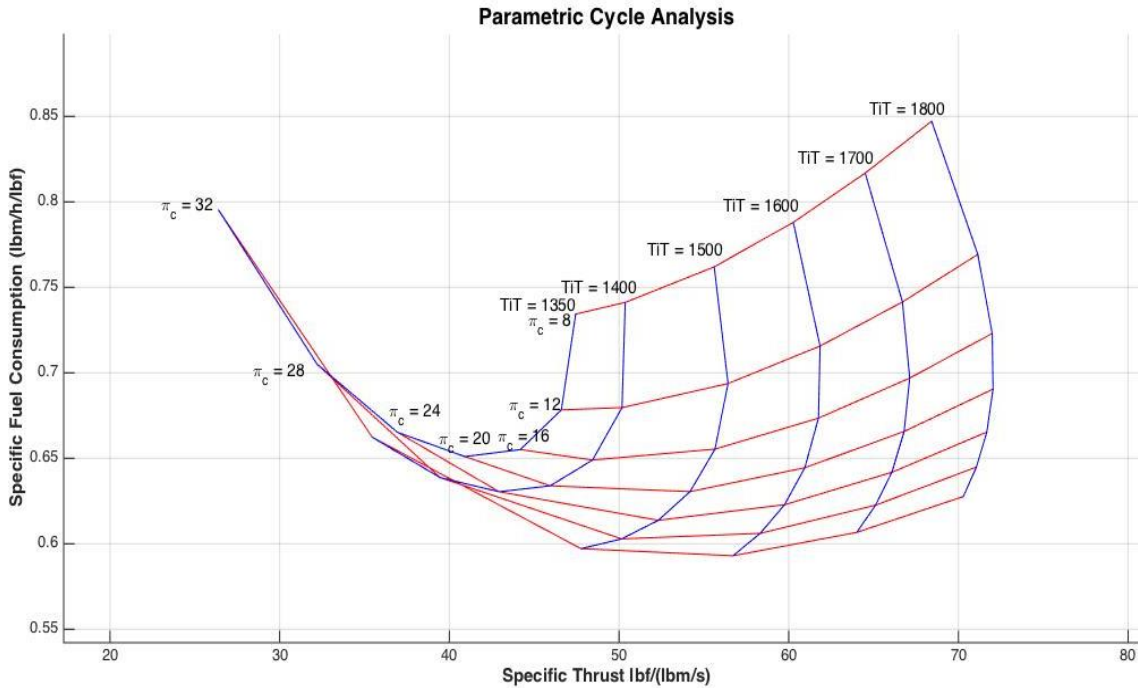


Figure 3.5 : Parametric Cycle Analysis (dry) – OPR vs TIT variation (BPR = 1.2)

The wet conditions of turbofan engine (afterburner is on) are important on the selection of design parameters. Therefore, evaluation of various afterburner values is going to be made. In order to do it, different cases of the design parameter of T_{17} – maximum afterburner temperature is calculated.

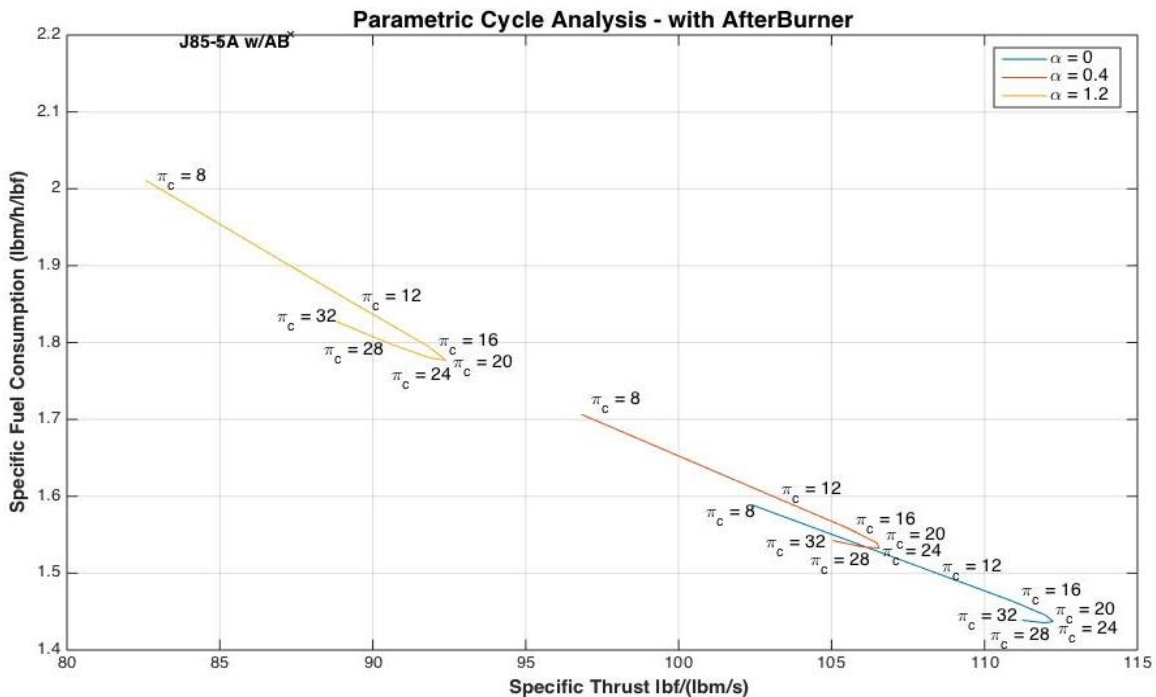


Figure 3.6 : Parametric Cycle Analysis (wet) – OPR & BPR Variation ($T_{17} = 2000\text{ K}$)

Specific thrust values in Figure 3.6 are higher than the baseline value, which needs to be optimized in order to reach out the most effective SFC result for wet condition. For this purpose, on the BPR of 1.2, variation of T_{17} is made to analyse the difference and effects. The new analysis has been made for 1600K, 1800K and 2000K.

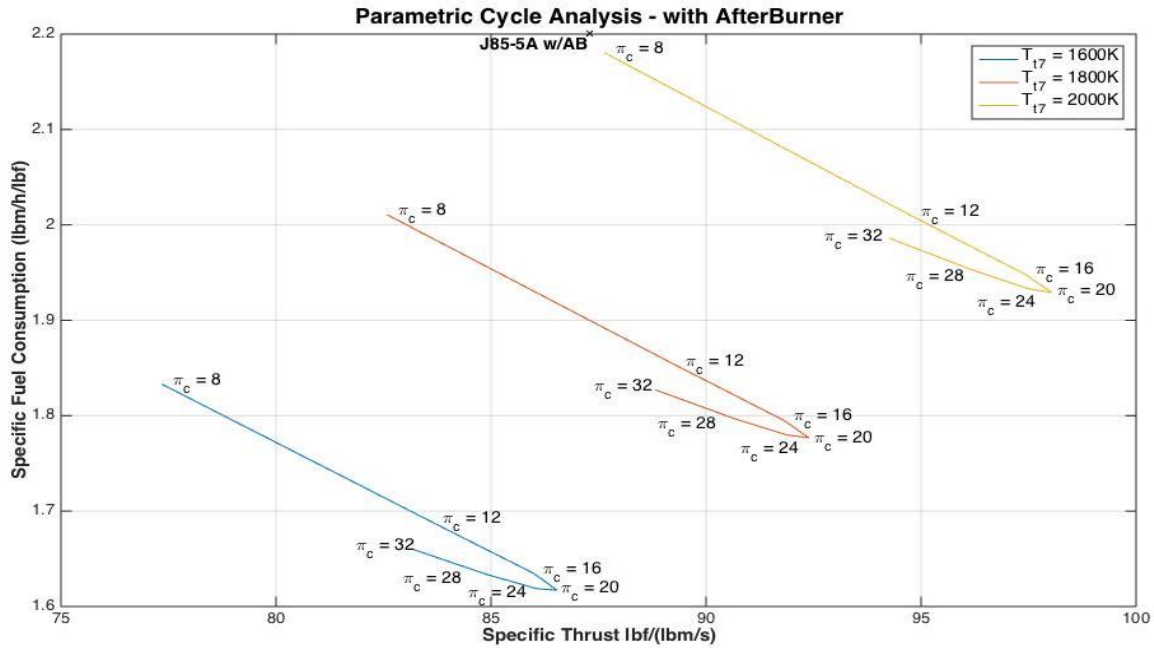


Figure 3.7 : Parametric Cycle Analysis (wet) – OPR & T_{t7} variation (BPR = 1.2)

For the wet condition, besides meeting the requirements of 4000lbf on the SLS condition, it is very important to reach out as low SFC as possible for new engine. Both 1600K and 1800K afterburner maximum temperature provide the required wet thrust value. On the other hand, according to the selected design parameters, the mass flow can be modified on compressor design phase. However, performance analysis is going to be made before to make sure new engine meets the all thrust requirements from RFP.

From the parametric cycle analysis evaluation, the initial design preferences are selected as accordingly:

Table 3.2 : Primary Design Selection Values

Primary Selected Design Values			
ByPass Ratio		1.2	
Fan Pressure Ratio		2.3	
Compressor Pressure Ratio		16	
Dry Condition		Wet Condition	
T_{t4} (K)	1500 (2700° R)	T_{t7} (K)	1800 (3240° R)
Specific Thrust lbf/(lbm/s)	55.29	Specific Thrust lbf/(lbm/s)	93.71
SFC (lbm/h)/lbf	0.66	SFC (lbm/h)/lbf	1.76

On the design, rather than sizing engine with required thrust values on each mission step, main priority of our design is to improve the performance and flight capabilities of the new engine. The diameter of the baseline engine is already quite small, therefore stronger new design with similar size is preferred. Thanks to higher technological limits, potentially increased engine RPM enables 50 lbf/s mass flow with 9 in fan diameter to be chosen for the new design.

Lastly, basic comparison of specific thrust vs mass flow is made with baseline engine.

Table 3.3 : Parametric Cycle Analysis (at SLS) Summary in Wet Condition

Parametric Cycle Analysis Summary (w/AB)			
Station Number	Stagnation Pressure (psia)	Stagnation Temperature (°R)	Mass Flow (lbm/s)
0	14.70	545.67	50.00
1	14.70	545.67	50.00
2	14.11	545.67	50.00
2.5	32.46	712.94	21.82
13	32.46	712.94	27.27
3	225.79	1315.80	21.82
4	216.76	2700.00	23.01
4.5	77.14	2115.74	23.01
5	37.61	1798.98	23.01
16	32.46	712.94	27.27
6A	36.12	1166.30	50.28
7	34.31	3240.00	52.08
9	33.63	3240.00	52.08

3.3. Sensitivity Analysis

In order to evaluate effect of each design parameter on the new engine, a sensitivity analysis is conducted.

Table 3.4 : Sensitivity Analysis

Sensitivity Analysis					
Parameter	Range	Dry		Afterburner	
		Specific Thrust (lbf/(lbm/s))	TSFC (lbm/s/(lbf))	Specific Thrust (lbf/(lbm/s))	TSFC (lbm/s/(lbf))
T_{t4} (K)	1400 - 1800	1.732	0.377	1.158	-0.802
T_{t7} (K)	1600 - 2000	-	-	0.532	0.765
π_c (OPR)	12 - 20	0.004	-0.194	0.057	-0.066
π_f (FPR)	2.2 - 2.8	-0.275	0.298	-0.299	0.320
α (BPR)	0.6 - 1.2	-0.238	-0.081	-0.055	0.058
M_{cruise}	0.7 - 0.9	-0.535	0.374	-	-
M_{max}	1.2 - 1.5	-	-	-0.563	0.057

3.4. Performance Analysis Evaluation

On the performance analysis, other required conditions are going to be evaluated and checked if new engine fits all the flight conditions. For this purpose, different flight envelopes, altitudes and mach numbers with various throttle and afterburner settings will be analysed.

The main part of the engine whose operation limits change the least is the turbine stage. Both HPT and LPT stages operation values of pressure and temperature ratios vary very low with the different flight conditions, which can be neglected and assumed as same since both turbines are going to be designed as choking. From the Farokhi [6] source, own program for performance analysis is developed appendix A and compared with the AEDsys program results.

On this stage of analysis, mass flow is considered as 50 lbm/s in order to improve performance of the engine and evaluated in the next in-depth analysis section.

Table 3.5 : Performance Analysis Results

Performance Analysis Results					
Condition	Loiter	Cruise	Max. Velocity		
	Dry	Dry	Wet		
M₀	0.5	0.85	1.3	1.4	1.5
Mass Flow	34	20	24.30	27.17	30.47
π_f (FPR)	2.305	2.305	2.31	2.31	2.31
π_c (OPR)	16	16	16	16	16
α (BPR)	1.202	1.202	1.21	1.21	1.21
T_{t4} (R)	1341.6	1238.8	1433.2	1490.9	1553.2
T_{t7} (R)	-	-	1800	1800	1800
η_{Thermal}	37.52%	42.84%	35.43%	37.16%	38.88%
η_{Propulsive}	44.93%	59.39%	49.45%	51.26%	52.97%
η_{Overall}	16.85%	25.44%	17.52%	19.05%	20.59%
F_{specific} (lbf/(lbf/s))	40.33	35.21	93.58	94.24	94.79
TSFC (lbf/h/(lbf))	0.78	0.81	1.78	1.77	1.75
F (lbf)	1371.18	704.29	2274.03	2560.21	2880.02
F_{required} (lbf)	1230	635	1500	-	-

3.5. In-Depth Analysis for Engine Design

In order to design the most efficient engine for certain mission profile and requirements, fuel consumption, cruise TSFC and engine weight need to be deeply analysed. As RFP requested in-depth analysis on these matters, we are going to go through certain number of calculations and make comparisons for evaluating our design values.

With the developed performance cycle analysis program and AEDsys program of Mattingly [4], following list of measurements are obtained.

3.5.1. Mission Fuel Burn Analysis

In the AEDsys programme, we have registered the developed mission profile for T38. Over 70 analyses for different type of engines are evaluated for new T38 and compared. On the all analyses, take off weight is taken as 11050 lbf and T_{t7} as 3240 R°.

It is important to compare the FPR and BPR ratios and their effect on fuel consumption while keeping the total compressor stages in mind. Baseline turbojet engine has 9 compressor stages, therefore the maximum stages considered should not be higher than it.

Apart from FPR and OPR comparisons, T_{t4-max} and BPR are also very important for the mission profile. Comparison of as many analyses as possible are useful for the evaluation of design values for the new engine.

Table 3.6 : Mission Fuel Burn – In-depth Analysis I

<u>Analysis #</u>	<u>OPR</u>	<u>FPR</u>	<u>HPR</u>	<u>BPR</u>	<u>T₄ (R)</u>	<u>W_{Fuel} (lbm)</u>	<u>W_{final} (lbm)</u>	<u>Compressor</u>	<u>∑ Stage #</u>	<u>T_{SLs} (lbf)</u>
1	12	2.3	5.22	1.569	2700	2880	8170	2F - 5H	7	4309
2		2.6	4.62	1.05		2879	8171	2F - 5H	7	4644
3		2.9	4.14	0.687		2911	8139	3F - 4H	7	4917
4		3.2	3.75	0.42		2956	8094	3F - 4H	7	5146
5		3.5	3.43	0.2		3026	8024	3F - 4H	7	5406
6	16	2.3	6.96	1.685	2700	2793	8257	2F - 6H	8	4316
7		2.6	6.15	1.168		2764	8286	2F - 6H	8	4649
8		2.9	5.52	0.807		2777	8273	3F - 5H	8	4921
9		3.2	5.00	0.54		2806	8244	3F - 5H	8	5149
10		3.5	4.57	0.334		2844	8206	3F - 5H	8	5344
11	20	2.3	8.70	1.701	2700	2758	8292	2F - 7H	9	4320
12		2.6	7.69	1.195		2703	8347	2F - 7H	9	4653
13		2.9	6.90	0.841		2704	8346	3F - 6H	9	4924
14		3.2	6.25	0.58		2725	8325	3F - 6H	9	5151
15		3.5	5.71	0.378		2755	8295	3F - 5H	8	5346
16	24	2.3	10.43	1.664	2700	2748	8302	2F - 8H	10	4324
17		2.6	9.23	1.174		2669	8381	2F - 8H	10	4656
18		2.9	8.28	0.831		2661	8389	3F - 7H	10	4927
19		3.2	7.50	0.577		2677	8373	3F - 7H	10	5153
20		3.5	6.86	0.382		2702	8348	3F - 6H	9	5347

Table 3.7 : Mission Fuel Burn – In-depth Analysis II

<u>Analysis #</u>	<u>OPR</u>	<u>FPR</u>	<u>HPR</u>	<u>BPR</u>	<u>T₄ (R)</u>	<u>W_{Fuel} (lbm)</u>	<u>W_{final} (lbm)</u>	<u>Compressor</u>	<u>∑ Stage #</u>	<u>T_{SLs} (lbf)</u>
41	16	2.3	6.96	1.216	2520	2851	8199	2F - 6H	8	4331
42				1.654	2700	2823	8227			4330
43				2.095	2880	2852	8198			4328
44				2.538	3060	2855	8195			4326
45				2.984	3240	2853	8197			4324
46	16	2.3	6.96	2	2520	3441	7609	2F - 6H	8	3771
47					2700	2930	8120			4127
48				2880	2801	8249	4376			
49				2.75	3060	2853	8197			4233
50					3240	2739	8311			4410
51	24	3.5	6.86	0.088	2520	2846	8204	3F - 6H	9	5348
52				0.362	2700	2784	8266			5352
53				0.638	2880	2749	8301			5354
54				0.916	3060	2729	8321			5354
55				1.195	3240	2719	8331			5354
56	24	3.5	6.86	0.6	2520	2814	8236	3F - 6H	9	4732
57					2700	2761	8289			5113
58				2880	2748	8302	5387			
59				1.1	3060	2704	8346			5219
60					3240	2710	8340			5414

Results of 2 better engines; OPR 16 and 24 make the design preference hard for the new engine. On this point, FPR needs to be estimated as well in order to obtain better results for each OPR scenario.

Due to the optimized performance results, decreased stage number which means potential lower weight, OPR of 16 seems a better design choice.

Table 3.8 : Mission Fuel Burn – In-depth Analysis III

<u>Analysis #</u>	<u>OPR</u>	<u>FPR</u>	<u>HPR</u>	<u>BPR</u>	<u>T₄ (R)</u>	<u>W_{Fuel} (lbm)</u>	<u>W_{final} (lbm)</u>	<u>Compressor</u>	<u>Σ Stage #</u>	<u>T_{SLS} (lbf)</u>
61	16	2.3	6.96	1.2	2520	2802	8248	2F - 6H	8	4351
62				1.4		2837	8213			4216
63				1.6		2900	8150			4082
64				1.8		3006	8044			3947
65				2		3282	7768			3811
66	16	2.3	6.96	1.2	2700	2750	8300	2F - 6H	8	4473
67				1.4		2755	8295			4471
68				1.6		2781	8269			4365
69				1.8		2808	8242			4252
70				2		2858	8192			4138
66	24	3.5	6.86	0.3	2700	2778	8272	3F - 6H	9	5431
67				0.6		2742	8308			5133
68				0.9		2716	8334			4843
69				1.2		2735	8315			4473

3.5.2. Cruise TSFC Analysis

Thanks to the MATLAB program we have developed, we are able to obtain the behaviours of the design parameters in cruise condition and create carpet plots to compare different values with each other. This extra analyses help us to choose the most suitable and efficient design selection for the new engine. Furthermore, we are going to evaluate results for cruise condition.

Similar to parametric cycle analyses, coherency between OPR and FPR, together with BPR is critical to provide an efficient TSFC for cruise. Initial design choices for new engine look very good for this condition. TiT effects on these parameters are also prominent, therefore further measurements are needed.

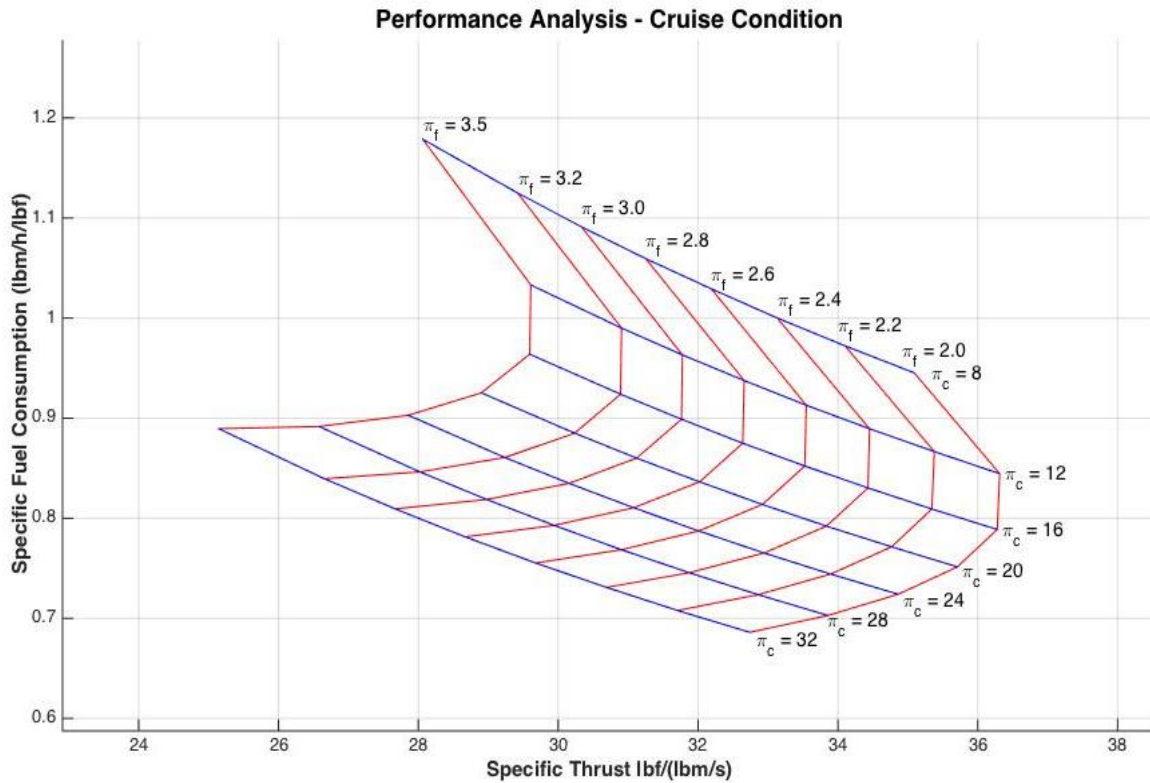


Figure 3.8 : Performance Analysis – Cruise Condition, OPR & FPR variation
(BPR = 1.2 & $TiT_{SLS} = 1500K$)

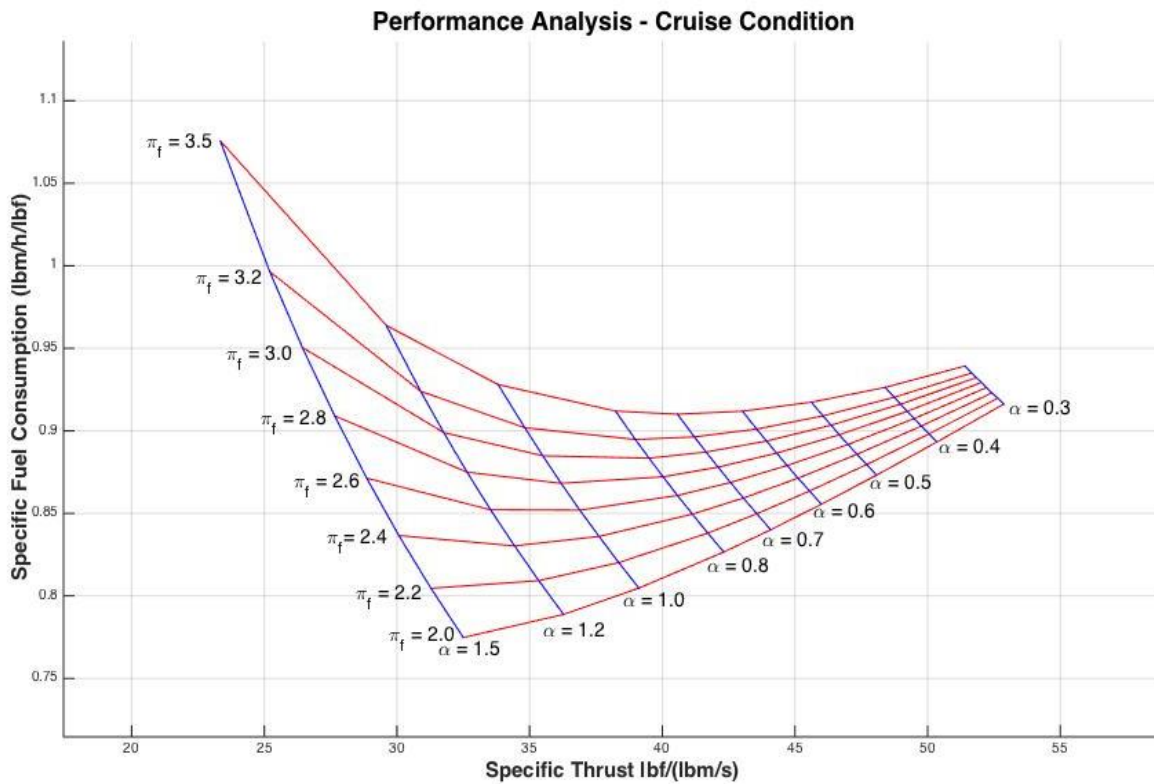


Figure 3.9 : Performance Analysis – Cruise Condition, BPR & FPR variation
(OPR = 16 & $TiT_{SLS} = 1500K$)

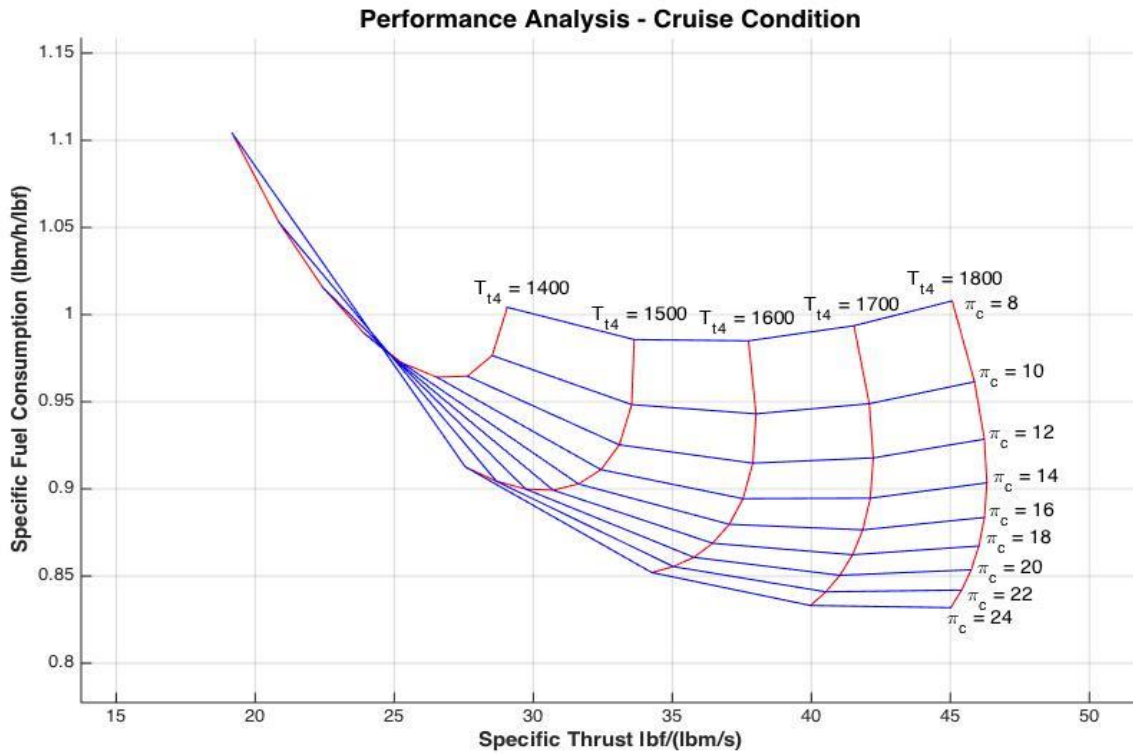


Figure 3.10 : Performance Analysis – Cruise Condition, OPR & TiT variation (BPR = 1.2)

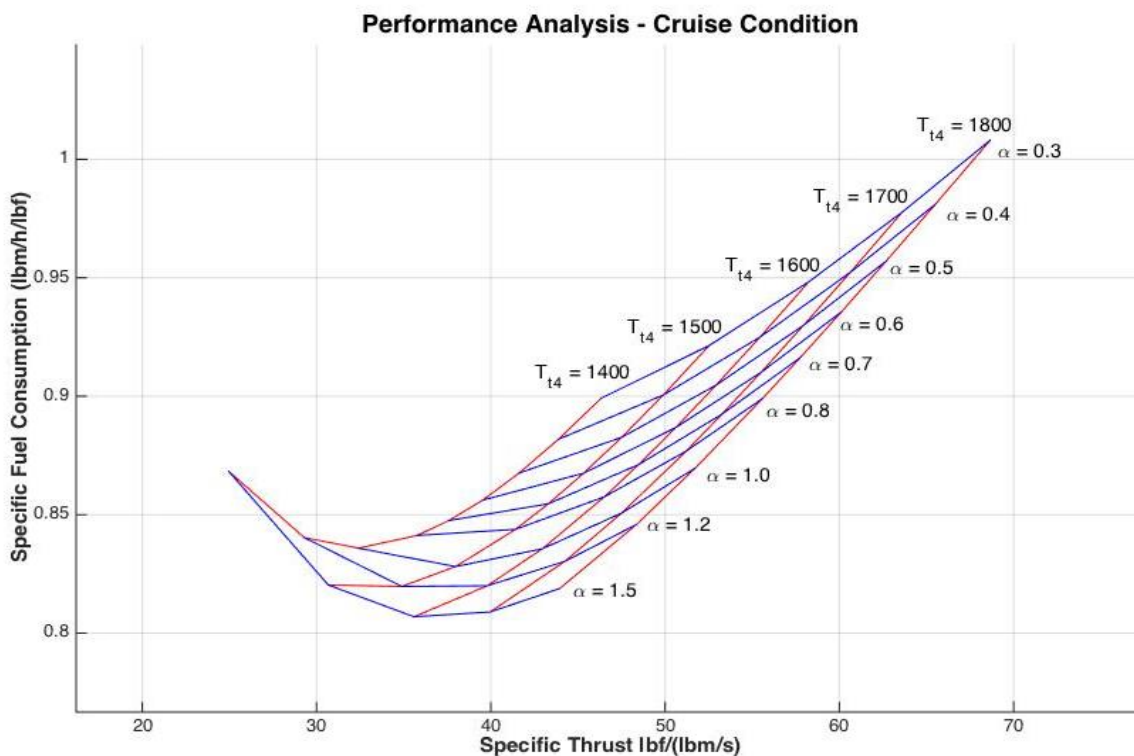


Figure 3.11 : Performance Analysis – Cruise Condition, BPR & TiT variation (OPR = 16)

According to the results from the off design analysis graphics on cruise condition, our design parameters selection provides quite good and efficient performances. Therefore, with the ensurance of the new engine weight, we can proceed with part designs.

3.5.3. Engine Weight Analysis

In order to analyse the engine weight and how design parameters have effect on it, a wide range of research is made about the methods and ways. Among the numerous applications and experiments that have been worked upon, one significant method seems to provide the most accurate results, which is WATE++ program that has been developed by NASA in collaboration with Boeing [7]. Since this entire program is not publicly available, a basic version has been found from the referenced MIT report. In this simpler version, the variables that effect directly the engine weight are OPR, BPR and mass flow.

$$W_{engine} = a * \left(\frac{\dot{m}_{core}}{100}\right)^b * \left(\frac{OPR}{40}\right)^c$$

Current technology (late 1990's through mid 2000s):

$$a = (-6.590 \times 10^{-1}) BPR^2 + (2.928 \times 10^2) BPR + 1915$$

$$b = (6.784 \times 10^{-5}) BPR^2 - (6.488 \times 10^{-3}) BPR + 1.061$$

$$c = (-1.969 \times 10^{-3}) BPR + 0.0711$$

Advanced materials (including carbon composites, CMC, MMC, and TiAl):

$$a = (-6.204 \times 10^{-1}) BPR^2 + (2.373 \times 10^2) BPR + 1702$$

$$b = (5.845 \times 10^{-5}) BPR^2 - (5.866 \times 10^{-3}) BPR + 1.045$$

$$c = (-1.918 \times 10^{-3}) BPR + 0.0677$$

This version of the estimation is used for geared turbofan engines. Since the ideology of this formula and method is similar, we are going to measure the accuracy of the function with similar mixed flow turbofan engines.

Table 3.9 : Weight Estimation Comparison – 5th Generation Fighters

Engine Name	P&W F119-PW-100	P&W F135	AL-31F	IHI Corporation XF5
Airflow (lbm/s)	270	307.8	243	100
OPR	26.8	28	23	26
ByPass Ratio	0.45	0.57	0.57	0.39
W _{Real} (lbm)	3900	3750	3373	1420
W _{Estimation} (lbm)	3841.56	3617.09	3178.18	1389.20
Error %	1.50	3.54	5.78	2.17

Table 3.10 : Weight Estimation Comparison – Jet Trainers

Engine Name	GE F404	AI-222-25F	Tumansky R-13	AI-222-25
Airflow (lbm/s)	146	109.57	145.5	109.57
OPR	26	15.43	8.9	15.43
ByPass Ratio	0.34	1.19	0	1.19
W _{Real} (lbm)	2282	1190	2656	970
W _{Estimation} (lbm)	2140.05	1021.74	2561.90	1021.74
Error %	6.22	14.14	3.54	5.33

Except the AI-222-25F engine, the error percentage is below maximum 6.22. The basic formula from WATE++ and MIT report seems to be feasible to make analyses and implement for the new designed engine.

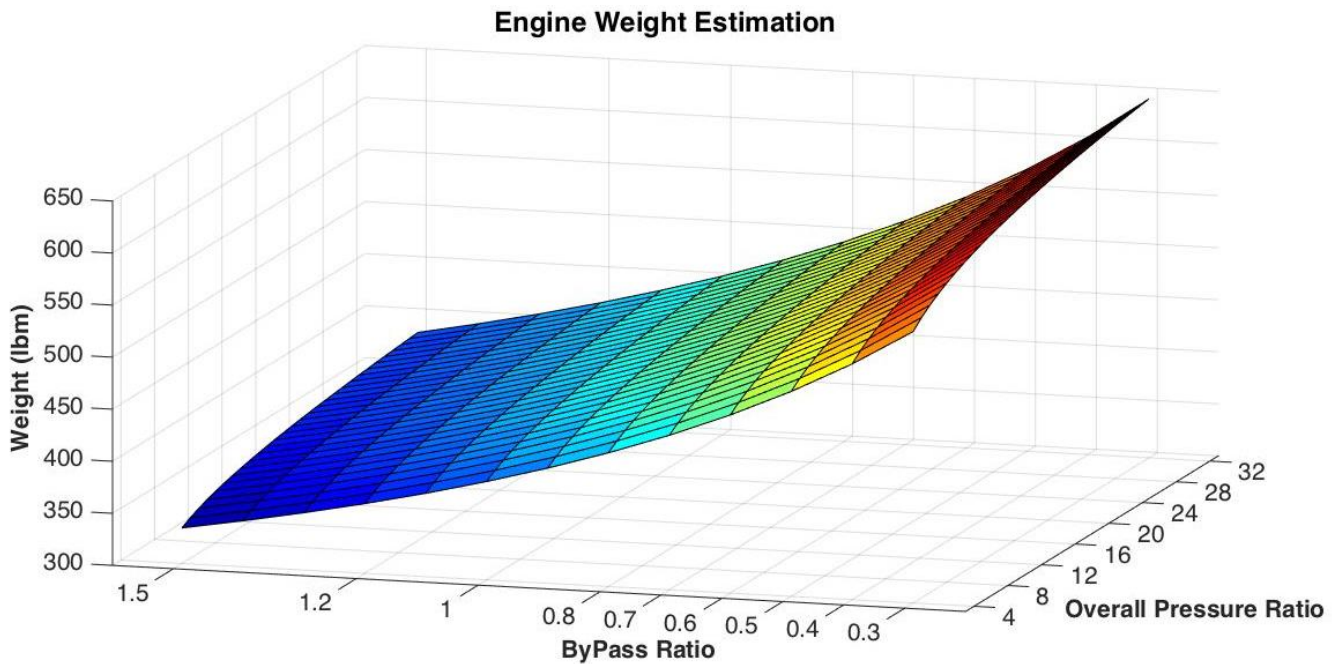


Figure 3.12 : Estimated Engine Weight Variation (Mass Flow = 50 lbm/s)

Two most significant engine types are compared in order to evaluate the choice.

Table 3.11 : New Engine Design Options Weight Estimation Comparison

Engine Options	Engine #1	Engine #2
Airflow (lbm/s)	50	50
OPR	16	24
ByPass Ratio	1.2	0.6
$W_{\text{Estimation}}$ (lbm)	401.78	530.79

With the new engine design parameters preference, new engine weight is approximately calculated in Table 3.10. With the 5.28% average error margin that was measured from other weight estimations comparison, new engine weight is calculated as:

Table 3.12 : BeEngine vs J85-5A

Engines	<u>J85-GE-5A</u>	<u>BeEngine</u>
Weight (lbm)	584	424.2
Weight (kg)	264.90	192.41

4. COMPRESSOR DESIGN

1st step to start designing parts of the new engine is to determine and optimize its compressor. After reaching certain values on parametric cycle and off-design analyses, design of the compressor that meets its cycle values is extremely important. By improving the baseline engine of GE J85-5A, design of 2 spool low-bypass turbofan engine will be worked upon.

For fan/LPC stage, constant tip line, repeating row, repeating stage design is found appropriate, while for HPC constant mean line, repeating row and repeating stage design is chosen. Both calorically perfect gas and ideal gas properties of air will be used in order to reach the most accurate values. Furthermore, swirl angles assumed as constant and free vortex swirl model has been used.

Inlet Mach number selected as 0.58, which is decided as the most optimum inlet velocity for the small size of engine in order to be strong and efficient in its all parts. On the other hand, with the increased engine entrance area (higher hub to tip ratio on engine 1st stage compressor), the mass flow is aimed to be increased by $\approx 15\%$ to reach out the 1st estimation of $\approx 50\text{lbm/s}$. Besides, the Mach number before combustion becomes 0.36, which is a good and efficient number, especially for the ultimate technology and newly developed combustion chambers.

Technology in the aviation has reached an ultimate level to allow diffusion factor value as 0.55. By the evaluation of the aimed design values, solidity ratios 1.1 for fan and 1.5 for HPC are selected. The reason behind the high HPC solidity ratio is the goal of highest fuel consumption for a potential new engine. Because of the significant performance damage of very high solidity ratios, 1.5 is a good combination of intense and successful HPC chapter.

Other minor design parameters of Flow Coefficient, Stage Loading Factor, Degree of Reaction and De Haller Criterion are going to be constantly checked in all parts of compressor design to ensure the efficiency and reality of the design.

As last, RPM of the fan/LPC is selected in a comparison with the real value of baseline engine, because of the better technology opportunities and 2-spool new design. Besides, counter rotating spool design is selected due to its benefits in moment balance and power.

4.1. Fan Design & Calculations

On the parametric cycle and off design analyses, low fan pressure ratio design method is decided in order to reach the lowest specific fuel consumption while achieving the required thrust points. The initial design value for fan/LPC, 2.3 pressure ratio is going to be aimed.

Taper ratio is selected as 0.8 for ensuring the stress safety of the blades. Besides, hollow fan blades would be useful on this part for both meeting the stress and low weight needs.

Last of all, inlet guide vane (IGV) is added due to its contribution to fan operations.

Table 4.1 : Fan Design Parameters & Values

Fan Design Parameters	
Number of Stages	2
Mass Flow Rate (lbm/s)	~ 50
Rotor Angular Speed (rad/s)	~ 1840
Inlet Total Pressure (lbf/ft ²)	2032.128
Inlet Total Temperature (K)	303.15
Entry Angle (degrees)	28.5
Entry Mach	0.58
Diffusion Factor	0.55
Polytropic Efficiency	0.89
Solidity	1.1
Exit Angle for Last Stage (degrees)	28.5
Exit Mach	0.50
Ratio of Specific Heat for Part	1.4
Inlet Diameter (ft - in)	1.5 - 18
Initial Hub to Tip Ratio	0.45
Design Choice	Constant tip

Table 4.2 : Fan Design Output Values – Fan Stages 1 & 2

Fan Measurements	Stage 1			Stage 2		
Total Temperature (K)	303.15	349.72	349.72	349.72	396.29	396.29
Total Temperature (°R)	545.67	629.50	629.50	629.50	713.33	713.33
Static Temperature (K)	284.04	302.24	330.61	330.61	351.25	377.18
Static Temperature (°R)	511.27	544.03	595.10	595.10	632.25	678.93
Total Pressure (psia)	14.11	22.23	22.03	22.03	32.93	32.51
Static Pressure (psia)	11.24	13.43	18.09	18.09	21.58	27.35
Mach	0.58	0.88	0.54	0.54	0.80	0.50
Velocity (ft/s)	647.51	1006.80	647.51	647.51	959.21	647.51
Mean Radius (in)	6.53	6.90	7.41	7.41	7.62	7.87
Flow Area (in ²)	202.94	182.11	148.05	148.05	131.94	112.10
Hub to Tip Ratio	0.45	0.53	0.65	0.65	0.69	0.75
Total Temperature Increase (K - R)	46.57 - 83.83			46.57 - 83.83		
Stage Total Temperature Ratio	1.15			1.13		
Stage Total Pressure Ratio	1.56			1.48		
de Haller Criteria	0.68			0.80		
Flow Coefficient	0.57			0.50		
Stage Loading	0.38			0.46		
Reaction Factor	0.46			0.52		
Rotor Mean Speed (ft/s)	1000.00			1135.64		
Tip Mach Number	1.34			1.25		
Mean Mach Number	0.90			0.95		
Total Temperature Ratio	1.31					
Total Pressure Ratio	2.30					

Important design limits of flow coefficient, stage loading and De Haller Criterion are all met with allowable margins. Tip Mach number is around 1.3, which is a common value for military aircraft engines. The tip supersonic velocity would be taken under control with twist angle through the end of fan blades. Moreover, degree of reaction value of both fan stages are around 0.5, which is highly satisfactory for both stages to share the burden of the static temperature rise. By all the calculations, successful diffusion factor is proven.

4.2. High Pressure Compressor Design & Calculations

Most of the fan/LPC assumptions are also valid for HPC design. The major difference is on the design type, which constant mean line method is used for this part as the reason of lower relative mean radius and easier repeating stages design. Besides, due to the separation of bypass and main core of the engine, this method is easier to produce and establish for new engine model without extra length or weight requirements.

Mean radius design method is selected with 0.45 feet (5.4 in). The reason of this selection is to meet the structural balance between core and bypass sides of the engine, high pressure spool RPM because of the operational limits which are closer to central lines and area/length optimization of new engine.

On the next steps, comparisons of both fan – low pressure turbine and high pressure compressor – high pressure turbine are going to be made to ensure the working balance between components by most efficient common RPMs and created / supplied power.

Table 4.3 : High Pressur Compressor Design Parameters & Values

High Pressure Compressor Design Parameters	
Number of Stages	6
Mass Flow Rate (lbm/s)	~ 23
Rotor Angular Speed (rad/s)	2700
Inlet Total Pressure (lbf/ft ²)	4635
Inlet Total Temperature (K - R)	392 – 705.6
Entry Angle (degrees)	26.8
Entry Mach	0.50
Diffusion Factor	0.55
Polytropic Efficiency	0.90
Solidity	1.5
Exit Angle for Last Stage (degrees)	26.8
Exit Mach	0.36
Ratio of Specific Heat for Part	1.39
Inlet Mean Radius (ft - in)	0.45 – 5.4
Initial Hub to Tip Ratio	0.75
Design Choice	Constant mean

Table 4.4 : High Pressure Compressor Output Values – Stages 1/2

<u>HPC Measurements</u>	<u>Stage 1</u>			<u>Stage 2</u>			<u>Stage 3</u>		
Total Temperature (K)	392.33	447.33	447.33	447.33	502.32	502.32	502.32	557.31	557.31
Total Temperature (°R)	706.20	805.19	805.19	805.19	904.18	904.18	904.18	1003.16	1003.16
Static Temperature (K)	374.17	402.61	429.16	429.16	457.02	484.16	484.16	513.06	539.15
Static Temperature (°R)	673.50	724.71	772.49	772.49	822.64	871.48	871.48	923.51	970.47
Total Pressure (psia)	32.19	49.11	48.84	48.84	71.27	70.60	70.60	99.13	98.23
Static Pressure (psia)	27.23	34.02	42.19	42.19	51.52	61.99	61.99	74.54	87.38
Mach	0.50	0.76	0.46	0.46	0.71	0.44	0.44	0.70	0.41
Velocity (ft/s)	628.77	996.92	628.77	628.77	996.92	628.77	628.77	996.92	628.77
Mean Radius (in)	5.40								
Flow Area (in ²)	57.60	47.65	41.11	41.11	35.58	31.47	31.47	27.58	24.85
Hub to Tip Ratio	0.73	0.77	0.80	0.80	0.82	0.84	0.84	0.86	0.87
Total Temperature Increase (K - R)	54.99 - 98.99			54.99 - 98.99			54.99 - 98.99		
Stage Total Temperature Ratio	1.14			1.12			1.11		
Stage Total Pressure Ratio	1.52			1.45			1.39		
de Haller Criteria	0.77								
Flow Coefficient	0.46								
Stage Loading	0.53								
Reaction Factor	0.54								
Rotor Mean Speed (ft/s)	1215.00								
Tip Mach Number	1.19			1.07			0.99		
Mean Mach Number	0.96			0.89			0.84		
Total Temperature Ratio	1.98								
Total Pressure Ratio	8.79								

Table 4.5 : High Pressure Compressor Output Values – Stages 2/2

<u>HPC Measurements</u>	<u>Stage 4</u>			<u>Stage 5</u>			<u>Stage 6</u>		
Total Temperature (K)	557.31	612.31	612.31	612.31	667.30	667.30	667.30	722.30	722.30
Total Temperature (°R)	1003.16	1102.15	1102.15	1102.15	1201.14	1201.14	1201.14	1300.13	1300.13
Static Temperature (K)	539.15	568.79	594.14	594.14	624.04	649.14	649.14	679.38	704.13
Static Temperature (°R)	970.47	1023.82	1069.46	1069.46	1123.27	1168.45	1168.45	1222.88	1267.44
Total Pressure (psia)	98.23	133.65	132.48	132.48	175.59	174.13	174.13	225.65	223.97
Static Pressure (psia)	87.38	103.58	119.11	119.11	139.23	157.96	157.96	182.55	204.70
Mach	0.41	0.63	0.39	0.39	0.60	0.38	0.38	0.57	0.36
Velocity (ft/s)	628.77	996.92	628.77	628.77	996.92	628.77	628.77	996.92	628.77
Mean Radius (in)	5.40								
Flow Area (in ²)	24.85	22.02	20.10	20.10	18.00	16.60	16.60	14.99	13.93
Hub to Tip Ratio	0.87	0.89	0.90	0.90	0.91	0.91	0.91	0.92	0.93
Total Temperature Increase (K - R)	54.99 - 98.99			54.99 - 98.99			54.99 - 98.99		
Stage Total Temperature Ratio	1.10			1.09			1.08		
Stage Total Pressure Ratio	1.35			1.31			1.29		
de Haller Criteria	0.77								
Flow Coefficient	0.46								
Stage Loading	0.53								
Reaction Factor	0.54								
Rotor Mean Speed (ft/s)	1215.00								
Tip Mach Number	0.92			0.86			0.81		
Mean Mach Number	0.79			0.75			0.71		
Total Temperature Ratio	1.98								
Total Pressure Ratio	8.79								

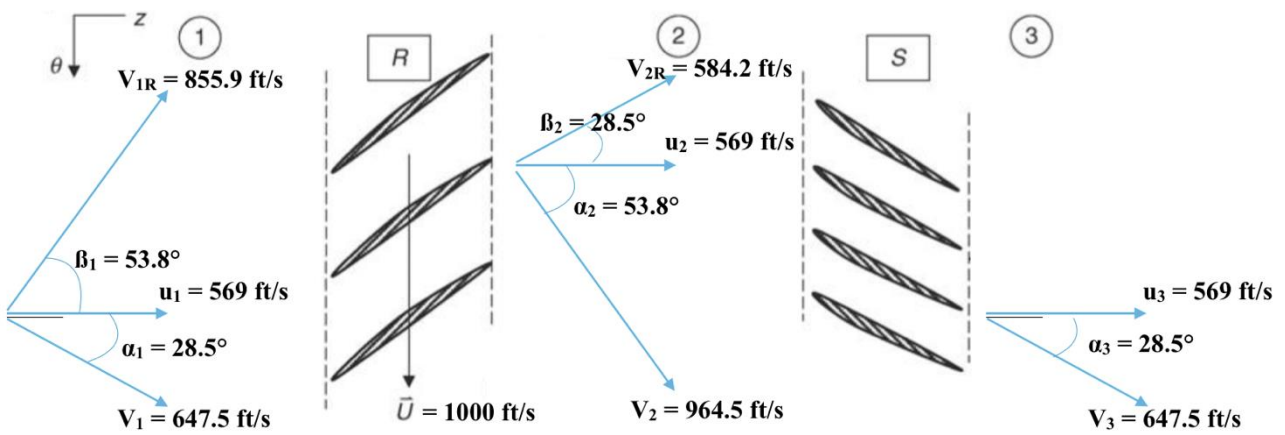


Figure 4.1 : Fan/LPC 1st Stage Velocity Triangles (mean)

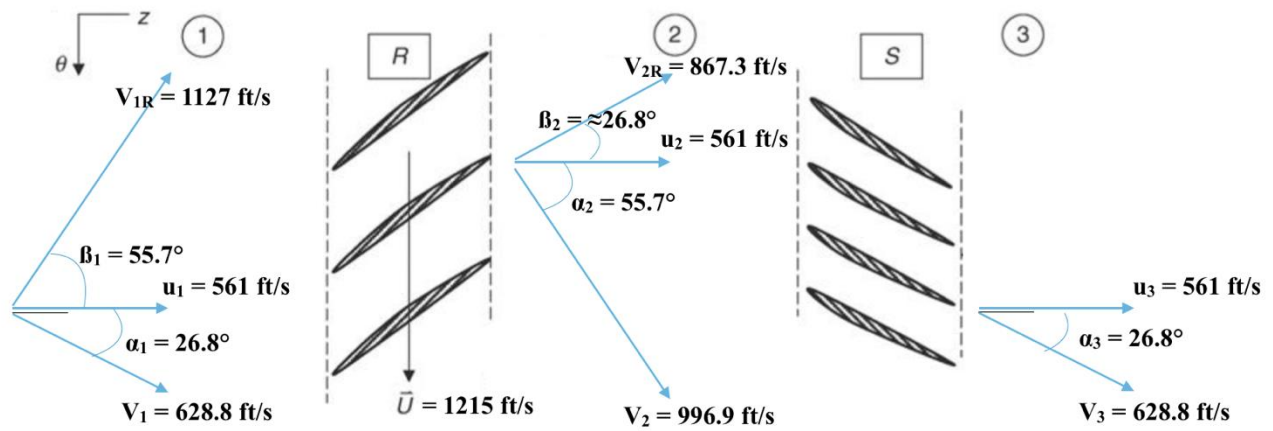


Figure 4.2 : HPC 1st Stage Velocity Triangles (mean)

4.3. Compressor Blade Geometry & Airfoil Selection

After the calculation of flow path and properties on both fan and high compressor sections, now we can evaluate more closely the movement of flow around the rotors and stators to select a suitable airfoil type for our engine.

Table 4.6 : Fan Repeating Design Stages Blade Angles (degree)

Fan Rotor Blade Angles			Fan Rotor Blade Angles		
α_1	-28.5	Flow Angle 1	α_2	-53.84	Flow Angle 1
α_2	-53.84	Flow Angle 2	α_3	-28.50	Flow Angle 2
i	2	Incidence Angle	i	-2	Incidence Angle
κ_1	55.84	Metal Angle 1	κ_1	-45.79	Metal Angle 1
δ^*	7.04	Deviation Angle	δ^*	-8.05	Deviation Angle
κ_2	35.54	Metal Angle 2	κ_2	-26.50	Metal Angle 2
φ	20.30	Chamber Angle	φ	-19.29	Chamber Angle
γ	41.69	Stagger Angle	γ	-36.15	Stagger Angle
$\Delta\beta$	25.34	Rotation Angle	$\Delta\beta$	-25.34	Rotation Angle
α_{AoA}	12.15	Angle of Attack	α_{AoA}	7.65	Angle of Attack

Table 4.7 : Fan Stages Blade Dimensions

Fan Blade Dimensions		Fan Rotor 1	Fan Stator 1	Fan Rotor 2	Fan Stator 2
Blade Mean Chord (in)	c	2.72	2.31	1.75	1.52
Axial Chord (in)	c_{axial}	2.03	1.87	1.31	1.22
Spacing (in)	s	2.48	1.78	1.59	1.17
Throat Opening (in)	o	1.46	1.56	0.94	1.02

Table 4.8 : HPC Repeating Design Stages Blade Angles (degree)

HPC Rotor Blade Angles			HPC Stator Blade Angles		
α_1	-26.8	Flow Angle 1	α_2	-55.74	Flow Angle 1
α_2	-55.74	Flow Angle 2	α_3	-26.80	Flow Angle 2
i	1	Incidence Angle	i	-1	Incidence Angle
κ_1	56.74	Metal Angle 1	κ_1	-47.85	Metal Angle 1
δ^*	7.90	Deviation Angle	δ^*	-7.89	Deviation Angle
κ_2	34.70	Metal Angle 2	κ_2	-25.80	Metal Angle 2
φ	22.04	Chamber Angle	φ	-22.05	Chamber Angle
γ	43.72	Stagger Angle	γ	-36.82	Stagger Angle
$\Delta\beta$	28.94	Rotation Angle	$\Delta\beta$	-28.94	Rotation Angle
α_{AoA}	12.02	Angle of Attack	α_{AoA}	10.02	Angle of Attack

Table 4.9 : HPC Stages Blade Dimensions

HPC Blade Dimensions		HPC Rotor 1	HPC Stator 1	HPC Rotor 2	HPC Stator 2	HPC Rotor 3	HPC Stator 3
Blade Mean Chord (in)	c	1.36	0.84	0.97	0.63	0.74	0.49
Axial Chord (in)	c_{axial}	0.98	0.67	0.70	0.50	0.54	0.39
Spacing (in)	s	0.91	0.56	0.65	0.42	0.49	0.33
Throat Opening (in)	o	0.51	0.50	0.36	0.37	0.28	0.29
		HPC Rotor 4	HPC Stator 4	HPC Rotor 5	HPC Stator 5	HPC Rotor 6	HPC Stator 6
Blade Mean Chord (in)	c	0.59	0.39	0.47	0.32	0.39	0.26
Axial Chord (in)	c_{axial}	0.42	0.31	0.34	0.25	0.28	0.21
Spacing (in)	s	0.39	0.26	0.32	0.21	0.26	0.18
Throat Opening (in)	o	0.22	0.23	0.18	0.19	0.15	0.16

The Cascade NACA graphics on Farokhi [6] shows that 2 airfoil types provide the required reactions and activities that are needed. Before making selection, close comparison of both airfoil types is important.

From the different solidity values and reaction of both airfoils, the ones with more performance and flexibility on various operation conditions are NACA 65-(18)10 and NACA 65-(12)10 airfoil types. Therefore, NACA 65-(18)10 is selected for fan stages and NACA 65-(12)10 is selected for HPC stages for reaching the best performance conditions.

For the stators, similar assumptions and design choices are going to be used.

4.4. Blade Number Measurement

In order to find the blade numbers for new engine, following assumptions are made:

Table 4.10 : Design and Assumption Values for Engine Rotor & Stator Blades

Blade Numbers Calculation Parameters	
Taper Ratio	0.8
IGV Solicity Ratio	0.55
Fan Rotor Solidity Ratio	1.1
Fan Rotor Chord / Height Ratio	0.55
Fan Stator Solidity Ratio	1.3
Fan Stator Chord / Height Ratio	0.55
HPC IGV Solicity Ratio	0.6
IGVs Chord / Height Ratio	0.3
HPC Rotor Solidity Ratio	1.5
HPC Rotor Chord / Height Ratio	0.6
HPC Stator Solidity Ratio	1.5
HPC Stator Chord / Height Ratio	0.6

With the measurements of the values, blade numbers for each stage found as followed:

Table 4.11 : Blade Numbers of Each Compressor Stage

Blade Numbers	Stator	Rotor
Inlet Guide Vane	-	15
1st Stage - Fan 1	16	23
2nd Stage - Fan 2	30	40
HPC - Inlet Guide Vane	-	40
3rd Stage - HPC 1	50	60
4th Stage - HPC 2	70	81
5th Stage - HPC 3	91	104
6th Stage - HPC 4	116	131
7th Stage - HPC 5	143	160
8th Stage - HPC 6	173	192

The IGV and fan blade numbers are as expected. On the other hand, the number of blades for HPC is gradually increasing, however quite high due to the high solidity number.

In order to clearly understand the importance and effect of the number of blades, blade stress calculations should be made. These calculations help designer to check the coherency of the assumptions and design values according to the material properties.

Besides, blade stress analysis is important for evaluating the required strength for the shaft of the engine, which is the main driver. Together with turbine calculations and reactions, we are going to obtain a high efficient power value.

4.5. Blade Stress Evaluation and Material Selection

Table 4.12 : Fan/LPC Blade Stress Calculations

Fan Blade Stress Calculations			
Stage 1		Stage 2	
W_{r1} (in)	2.02	W_{r3} (in)	1.31
W_{s2} (in)	1.51	W_{s4} (in)	1.31
h_1 (in)	4.95	h_3 (in)	3.18
h_2 (in)	4.20	h_4 (in)	2.75
A (in ²)	202.94	A (in ²)	148.05
σ_{c1} (psi)	40487.84	σ_{c2} (psi)	40773.01
AN ² (10 ¹⁰)	5.95	AN ² (10 ¹⁰)	5.98

Table 4.13 : HPC Blade Stress Calculations

HPC Blade Stress Calculations					
Stage 3		Stage 4		Stage 5	
W_{r5} (in)	0.56	W_{r7} (in)	0.41	W_{r9} (in)	0.32
W_{s6} (in)	0.47	W_{s8} (in)	0.36	W_{s10} (in)	0.28
h_5 (in)	1.70	h_7 (in)	1.21	h_9 (in)	0.93
h_6 (in)	1.40	h_8 (in)	1.05	h_{10} (in)	0.81
A (in ²)	57.60	A (in ²)	41.11	A (in ²)	31.47
σ_c (psi)	21199.05	σ_c (psi)	20297.25	σ_c (psi)	20059.13
AN ² (10 ¹⁰)	1.85	AN ² (10 ¹⁰)	1.77	AN ² (10 ¹⁰)	1.75
Stage 6		Stage 7		Stage 8	
W_{r11} (in)	0.25	W_{r13} (in)	0.20	W_{r15} (in)	0.17
W_{s12} (in)	0.22	W_{s14} (in)	0.18	W_{s16} (in)	0.15
h_{11} (in)	0.73	h_{13} (in)	0.59	h_{15} (in)	0.49
h_{12} (in)	0.65	h_{14} (in)	0.53	h_{17} (in)	0.44
A (in ²)	24.85	A (in ²)	20.10	A (in ²)	16.60
σ_c (psi)	19840.72	σ_c (psi)	19635.89	σ_c (psi)	19441.88
AN ² (10 ¹⁰)	1.73	AN ² (10 ¹⁰)	1.71	AN ² (10 ¹⁰)	1.70

Since both of the materials require high stress resistancy, Titanium Alloy (Ti-6Al-4V) for fan/LPC stages and Greek Ascoloy for HPC stages are potential materials. For fan/LPC, strength-to-weight ratio ~ 4.5 ksi/slug/ft³ corresponds to AN² value of 5.9×10^{10} in²-rpm² with a blade taper ratio of 0.8. From the graph of AN² function of specific stress and taper ratio [4]; Titanium Alloy (Ti-6Al-4V) is selected.

However, in order to decrease the weight & cost while increasing the stress tolerance, it is suggested to make mixture with other materials with higher axial and shear stresses tolerance.

5. TURBINE DESIGN

Turbine is the part where engine produces the required power to run its compressor, as well as rest of the operations of entire engine. Primary goal on this part is to design the turbine stage models according to the rest of the engine in order to meet the parametric on-design requirements, and also off-design operation conditions. For a given design, there is no best turbine design, rather it is a tradeoff of several parameters, such as efficiency, weight, power,

rotor stress, engine length and width limits, and of course cost. At the end, final turbine design should be an optimum solution for these parameters and RFP requirements.

Even though the baseline engine J85-GE-5A has 2 turbine stages, due to increased pressure ratio of new engine, design limitations must be checked. Considering the latest technology engines and comparison in between provide relevant source of information for the new case. Because of the major advantages, single stage HPT and LPT design is preferred.

Baseline engine has 2 turbine stages, which both of them are connected to 1 shaft on the baseline turbojet engine. New designed engine has 2 shafts, therefore both low pressure and high pressure turbines stages are going to be designed independently to meet LPC and HPC requirements. On the other hand, new engine has more than double of pressure ratio of the baseline engine and bypass ratio is included, therefore a brand new design is preferred. On the other hand, in order to overcome design challenges of turbine stages, HPT and LPT specifications are selected considering experiments and researches of various organizations, such as NASA and GE. At the end, the final design decisions and measurements are given following HPT and LPT sections.

For the HPT stage, cooling is preferred in a very low percentage of air due to its contribution to the component life and durability of material. Besides, cooling helps engine to have an extra control on the turbine inlet temperature, which is useful for various flight conditions and extreme throttle ratio scenarios of 5th generation aircrafts, such as high-g maneuvers and accelerations.

5.1. High Pressure Turbine (HPT) Design

Table 5.1 : High Pressure Turbine Design Point Parameters (0 M & Sea Level)

High Pressure Turbine Design Parameters					
τ_{tH}	0.80	$P_{t4.1}$ (lbf/ft ²) & psi	31538.63	γ_t	1.33
			219.02		
π_{tH}	0.358	$T_{t4.1-max}$ (K) & (°R)	1600	$g_c * c_p$ (ft ² /(s ² *°R))	6694.18
			2880		
N (rpm)	25783.10	\dot{m} (lbm/s)	23.20	R (ft*lbf/(lbm*°R))	57.38

On this step, a NASA report, Design and Cold-air Test of Single-Stage Uncooled Core Turbine with High Work Output [8] has taken into consideration for the future steps of design.

As it stated in the report, rim speed is higher than the suggested values in the literature due to the higher tip speed. Besides, RPM is also quite high, which is similar case to our new engine. After the calculations, we are going to compare the results with each other to check the feasibility of the design. As the design choice, mean line design has been conducted which is similar to NASA experiment.

For the design parameters of turbine, M_1 , M_2 and M_{3R} are used to make rest of the calculations. Besides, in order to shape the geometry of turbine, mean radius is selected as 0.5 ft (6 inch). Constant γ value of calorically perfect gas, ideal gas property of air and polytropic efficiency values are used into calculations. As last, u_3/u_2 is used as 0.9 to ensure the target of relative Mach number. Lastly, is $e_{tH} = 0.89$.

Design parameters and values are:

- Turbine entrance Mach Number: $M_1 = 0.3$

- HPT Vane Exit Mach Number: $M_2 = 1.15$ to ensure the choking flow
- HPT Rotor Exit Mach Number: $M_{3R} = 0.8$
- HPT Vane Exit angle: $\alpha_2 = 70^\circ$

M_2 is taken as supersonic to make sure flow is choked and M_{3R} is taken subsonic.

Table 5.2 : HPT Results – I (h: hub, m: mean, t: tip)

High Pressure Turbine		1h	1m	1t	2h	2m	2t	2Rm	3Rm	3h	3m	3t
T_t	K	1600.00			1586.05			1390.34	1359.94	1260.06		
	$^\circ R$	2880.00			2854.89			2502.62	2447.90	2268.10		
T	K	1576.59			1280.98	1301.95	1320.73	1301.95	1230.05	1229.7	1230.05	1230.55
	$^\circ R$	2837.86			2305.76			2343.51	2214.09	2213.46		
P_t	psia	219.02			218.39			128.44	106.63	78.41		
P		206.39			92.32	98.57	104.42	98.57	71.15	71.03	71.15	71.24
M	-	0.3			1.20	1.15	1.10	0.64	0.8	0.39	0.38	0.38
V	ft / s	791.89			2799.23	2705.07	2617.41	1508.86	1820.18	882.09	874.90	869.17
u		779.86			925.19			925.19	832.67	832.67		
v		137.51			2641.92	2541.93	2448.44	1191.93	1618.55	291.10	268.55	249.25
α	degrees	10.00			70.70	70.00	69.30	-	-	19.27	17.88	16.66
β		-			-			52.18	62.78	-		
r	ft	0.47	0.50	0.53	0.46	0.50	0.54	0.50	0.50	0.44	0.50	0.56
	inch	5.67	6.00	6.33	5.54	6.00	6.46	6.00	6.00	5.33	6.00	6.67
A	ft ²	0.17			0.24			-	-	0.35		
	in ²	25.00			35.03			-	-	50.83		

Stage loading, flow coefficient and efficiency are 3 parameters to check through the stage to make sure consistency between vane and rotor boundaries, which can be seen in Table 5.3.

Table 5.3 : HPT Results – II

Stage Loading	Flow Coefficient	Isentropic Efficiency	Aspect Ratio		Solidity		Blade Numbers	
			Vane	Rotor	Vane	Rotor	Vane	Rotor
1.684	0.578	0.902	1.000	1.000	0.969	1.353	55	55
					Preferred Design Choice			
					1.2	2	68	80

Cooled-turbine stage efficiency is 0.902. When compare this value with Smith Chart for turbine stage efficiencies [9], it seems consistent.

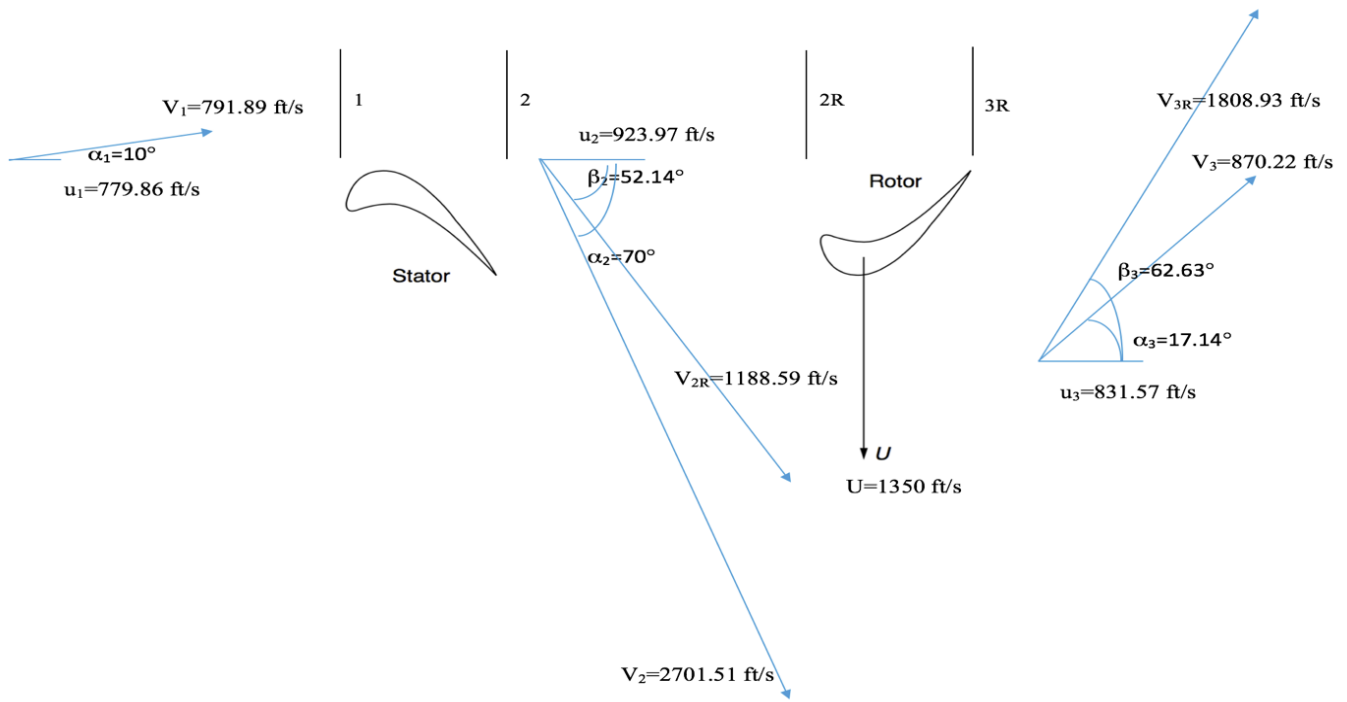


Figure 5.1 : HPT Stage Velocity Triangles (mean)

5.2. HPT Structural Analysis

After considering historical data for jet engine turbines, certain materials limit design choices. These materials will be inspected for further details of their strength, allowable RPMs and estimated working hours. With the maximum allowable stresses, maximum allowable shaft speed is determined by using the formula of AN^2 from Mattingly [4] which helps on finding allowable airfoil material specific strength.

Taper ratio (A_t/A_h) is selected as 0.7 since lower taper ratio enables blades to reduce stresses generated on turbine rotors [9]. The average annulus area (A) is 42.93 in². Also, to find out minimum rim web thickness, radial force balance equation is used. As a result, ratio rim web thickness over blade hub thickness becomes 0.56. The rotational speed (ω) is 2700 rad/s for High Pressure Turbine. Average Centrifugal stress (σ_{ave}) for turbine is found as 41.00 ksi.

Hot section of the engine, especially HPT stage is extremely important to be designed with well material and structural consistency. Ultimate technology materials, especially Ceramic Matrix Composites (CMC) [10] is a perfect solution for this case. With the developing production opportunities and chains of CMC, full turbine blades and other aircraft engine components are now possible [11] and will be even more in the close future [12]. Therefore, these important technological developments are considered for new engine.

CMC usage in engine provides not only strength, but also more efficiency and lighter body. For the engine design case, the most significant effects of CMC are the increased thrust, fuel consumption reduction and range improvements. Besides, engine cycles and durability will be quite improved comparing to the engines without CMC implementation [13]. Therefore, different versions of CMC, SiC/SiC, C/SiC and C/C look feasible for the blade selection [14]. Since Carbon Fiber Reinforced SiC CMCs are most promising material for hot section [15], it is selected for HPT vanes and rotor blades. It can also withstand the stress conditions of HPT stage without an issue considering the improvement on the material on upcoming 10 years. Moreover, even though C/SiC and C/C CMCs have better stress and temperature resistances, their oxidization ratios are less than SiC/SiC, especially conditions over 400°C [15].

Table 5.4 : HPT Stage Turbine Blade Measurements

1st Stage Turbine (HPT) Blade Stresses					
Blade Widths Vane			Blade Widths Rotor		
W_{vane} (ft - in)	0.058	0.695	W_{rotor} (ft - in)	0.094	1.131
h_1 (ft - in)	0.055	0.663	h_{2R} (ft - in)	0.077	0.929
h_2 (ft - in)	0.077	0.929	h_{3R} (ft - in)	0.112	1.348
Stress Calculations					
$W_{\text{dr}}/W_{\text{vane}}$	0.56		$W_{\text{dr}}/W_{\text{rotor}}$	0.56	
$W_{\text{dr-rim}}$ (ft - in)	0.032	0.39	$W_{\text{dr-rim}}$ (ft - in)	0.053	0.63
h_r / r_r	0.05		h_r / r_r	0.05	
r_r (ft - in)	0.45	5.40	r_r (ft - in)	0.42	5.07
ρ_1 (lbm/ft ³)	0.183		ρ_2 (lbm/ft ³)	0.11	
λ (taper ratio)	0.70		λ (taper ratio)	0.70	
A_1 (ft ² - in ²)	0.2433	35.0336	A_2 (ft ² - in ²)	0.353	50.8270
σ_c (psi)	43791.85		σ_c (psi)	38210.66	
A_{ave} (in ²)			42.93		
$\sigma_{c\text{-ave}}$ (psi)			41001.26		

Another important revolution CMC brings is on the HPT cooling phase. At the beginning of CMC implementation to engine hot stages, whether the need for cooling to HPT vanes and rotors is hard to estimate. In our case of maximum 1600K (2880 °R) turbine inlet temperature, cooling might not be needed since it is lower than the dangerous values of Carbon Fiber Reinforced SiC CMC. However, on this condition, low amount of cooling air seems feasible to ensure the sustainability of turbine stage [16], especially on the leading edges of HPT vane and rotor. Cooling air value of 3% in total seems appropriate.

From the Figure 5.2 below, 3% of coolant flow corresponds around 0.6-0.5 cooling effectiveness. In order to select a value and make comparison, experiment of Hess, Laminated Turbine Vane Design and Fabrication [17] is taken as an example.

Cooling air comes from the combustion entrance phase, where temperature is around 750K. 0.55 cooling effectiveness of 3% flow provides mean temperature decrease to $\approx 1100\text{K}$, which is sufficient enough to ensure the sustainability of HPT stage and its increased lifetime.

In order to ensure the reality of cooling effectiveness for on and off design conditions, as well as with the CMC properties on operational conditions, further experiments should be made. We aim to cool down leading edge of the stages since they reach the maximum heat flux and temperatures, therefore impingement and other leading edge cooling methods need to be investigated to be implemented in CMCs structure. For now, our assumptions with 10 years of development sufficient for the sustainability of new vanes and rotors.

As last, the vane and rotor creep life of CMC material is important for the durability and maintenance needs of our engine. On this phase, comparison of various CMC with Ni-based alloys which are used in engine components is made to obtain an estimated timeframe. Creep rate of Carbon Fiber Reinforced SiC CMCs are lower. However, in order to make sure the acceptability of the material applications on engine applications, total accumulated creep strain should be considered. With the variety of the stress that CMC goes through, the time for 1% creep strain would range roughly from 300h to 300 years, which is enough for most of the engineering applications that range from 100h to several 1000s hours [18], Figure 5.3.

Figure 5.2 : Leading Edge Turbine Cooling Effectiveness (Φ) [4]

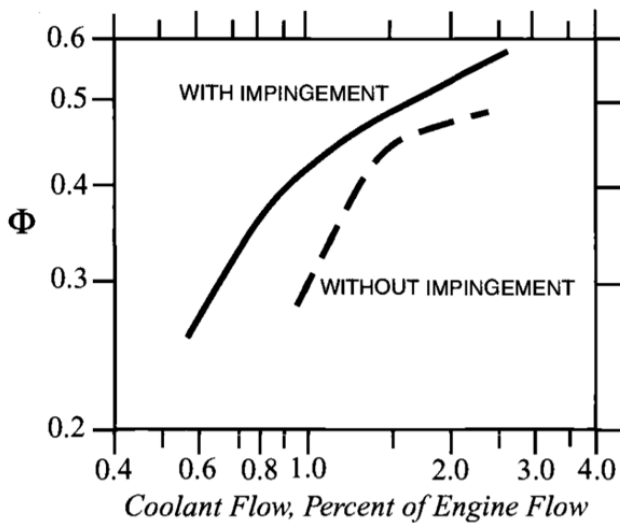
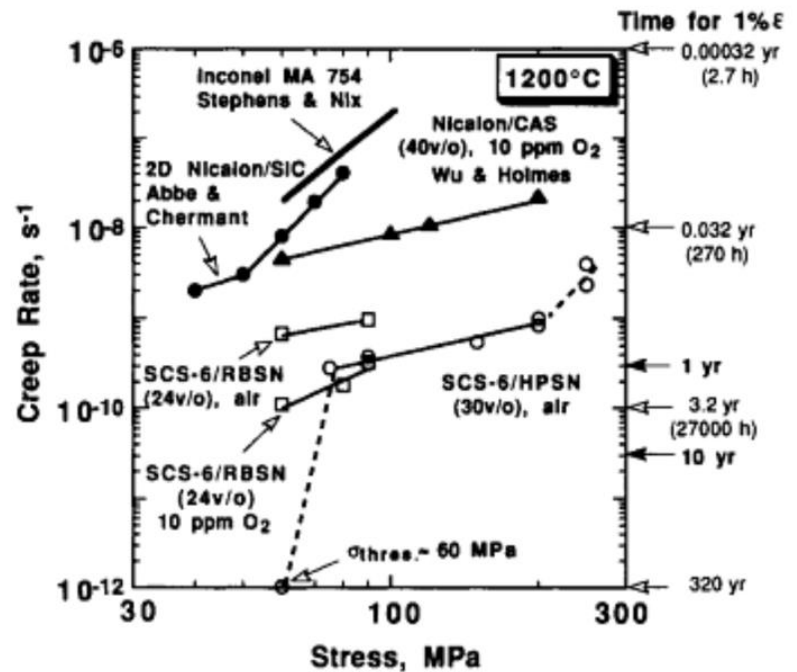


Figure 5.3 : Comparison of 100h tensile creep rate of various CMC at 1200°C with Ni-base superalloy MA754 [18]



5.3. Low Pressure Turbine (LPT) Design

Similar to HPT, after a research and comparison of similar military engines, 1-stage low pressure turbine is selected.

Table 5.5 : Low Pressure Turbine Design Point Parameters (0 M & Sea Level)

Low Pressure Turbine Design Parameters					
τ_{tL}	0.85	$P_{t4.5}$ (lbf/ft ²) & psi	11290.83 78.41	γ_t	1.33
π_{tL}	0.49	$T_{t4.5}$ (K) & (°R)	1260.06 2268.10	$g_c * c_p$ (ft ² /(s ² *°R))	6374.67
N (rpm)	17561.92	\dot{m} (lbm/s)	23.93	R (ft*lbf/(lbm*°R))	54.64

Design parameters and values are:

- LPT entrance Mach Number: $M_3 = 0.38$ from HPT exit condition
- LPT Vane Exit Mach Number: $M_4 = 1.10$ to ensure the choking flow
- LPT Rotor Exit Mach Number: $M_{5R} = 0.78$
- LPT Vane Exit angle: $\alpha_4 = 60^\circ$

u_3/u_2 is used again as 0.9 and is $e_{tL} = 0.90$.

Table 5.6 : LPT Results – I (h: hub, m: mean, t: tip)

Low Pressure Turbine		3h	3m	3t	4h	4m	4t	4Rm	5Rm	5h	5m	5t
T_t	K	1260.06			1260.06			1147.72	1127.62	1071.05		
	$^{\circ}\text{R}$	2268.10			2268.10			2065.89	2029.72	1927.89		
T	K	1230.05		1014.29	1050.35	1078.31	1050.35	1024.75	1023.59	1024.75	1025.54	
	$^{\circ}\text{R}$	2214.09		1825.72			1890.64	1844.55	1842.46			
P_t	psia	78.41			78.05			53.57	47.28	38.42		
P		71.15		32.55	37.47	41.66	37.47	32.15	32.01	32.15	32.25	
M	-	0.38		1.21	1.10	1.01	0.75	0.78	0.53	0.52	0.52	
V	ft / s	874.85		2461.86	2281.14	2128.61	1554.35	1594.18	1082.74	1069.50	1060.42	
u		861.56		1140.57			1140.57	1026.51	1026.51			
v		151.92		2181.71	1975.52	1797.25	1055.98	1219.70	344.39	300.16	266.00	
α	degrees	10		62.40	60.00	57.60	-	-	18.55	16.30	14.53	
β		-			-			42.79	49.92	-		
r	ft	0.45	0.50	0.55	0.44	0.50	0.56	0.50	0.50	0.42	0.50	0.58
	inch	5.35	6.00	6.65	5.23	6.00	6.77	6.00	6.00	5.06	6.00	6.94
A	ft ²	0.34		0.40			-	-	0.49			
	in ²	48.76		58.10			-	-	71.22			

Table 5.7 : LPT Results – II

Stage Loading	Flow Coefficient	Isentropic Efficiency	Aspect Ratio		Solidity		Blade Numbers	
			Vane	Rotor	Vane	Rotor	Vane	Rotor
1.822	0.638	0.917	1.000	1.000	0.997	1.753	30	44
					Preferred Design Choice			
					1.2	2	36	50

Stage loading, flow coefficient and isentropic efficiency are checked to ensure consistency between vane and rotor boundaries. Un-cooled turbine stage efficiency is 0.917.

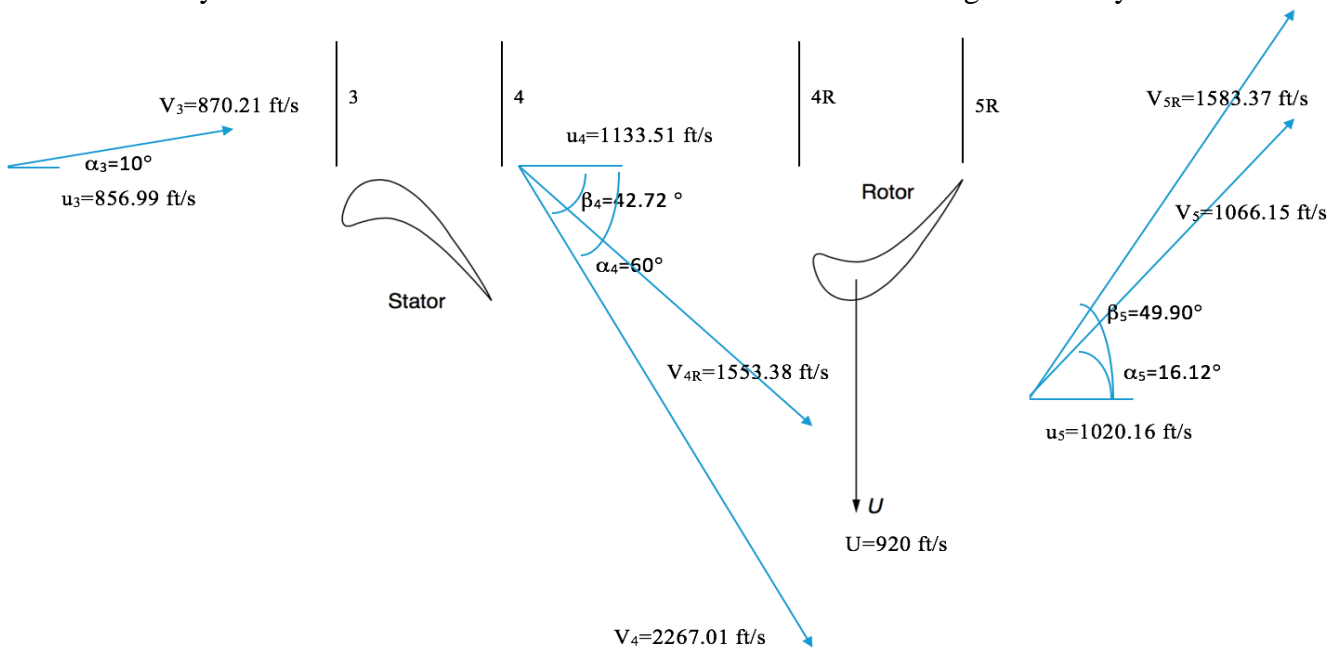


Figure 5.4 : LPT Stage Velocity Triangle (mean)

5.4. Turbine Blade Geometry

After the flow properties are determined, turbine blade geometries can be calculated.

Table 5.8 : HPT Stage Blade Geometries

HPT Nozzle Blade Profile			HPT Rotor Blade Profile		
α_1	10	Flow Angle 1 (°)	β_2	-52.18	Flow Angle 2 (°)
α_2	-70.00	Flow Angle 2 (°)	β_3	62.78	Flow Angle 3 (°)
i	-5	Incidence Angle (°)	i	-5	Incidence Angle (°)
κ_1	15.00	Metal Angle 1 (°)	κ_1	-47.18	Metal Angle 1 (°)
δ^*	3.33	Deviation Angle (°)	δ^*	2.18	Deviation Angle (°)
κ_2	-73.33	Metal Angle 2 (°)	κ_2	60.59	Metal Angle 2 (°)
φ	88.33	Chamber Angle (°)	φ	107.77	Chamber Angle (°)
γ	-29.17	Stagger Angle (°)	γ	6.71	Stagger Angle (°)
$\Delta\theta_{ind}$	17.40	Induced Flow Angle (°)	$\Delta\theta_{ind}$	22.64	Induced Flow Angle (°)
α_{AoA}	-40.83	Angle of Attack (°)	α_{AoA}	56.07	Angle of Attack (°)
c	0.66	Blade Mean Chord (in)	c	0.93	Blade Mean Chord (in)
c_{axial}	0.58	Axial Chord (in)	c_{axial}	0.92	Axial Chord (in)
s	0.55	Spacing (in)	s	0.46	Spacing (in)
o	0.19	Throat Opening (in)	o	0.44	Throat Opening (in)

Table 5.9 : LPT Stage Blade Geometries

LPT Nozzle Blade Profile			LPT Rotor Blade Profile		
α_3	10	Flow Angle 3 (°)	β_4	-42.79	Flow Angle 4 (°)
α_4	-60.00	Flow Angle 4 (°)	β_5	49.92	Flow Angle 5 (°)
i	-5	Incidence Angle (°)	i	-5	Incidence Angle (°)
κ_1	15.00	Metal Angle 1 (°)	κ_1	-37.79	Metal Angle 1 (°)
δ^*	2.29	Deviation Angle (°)	δ^*	0.79	Deviation Angle (°)
κ_2	-62.29	Metal Angle 2 (°)	κ_2	50.71	Metal Angle 2 (°)
φ	77.29	Chamber Angle (°)	φ	88.50	Chamber Angle (°)
γ	-23.65	Stagger Angle (°)	γ	6.46	Stagger Angle (°)
$\Delta\theta_{ind}$	17.40	Induced Flow Angle (°)	$\Delta\theta_{ind}$	20.76	Induced Flow Angle (°)
α_{AoA}	-36.35	Angle of Attack (°)	α_{AoA}	43.46	Angle of Attack (°)
c	1.29	Blade Mean Chord (in)	c	1.54	Blade Mean Chord (in)
c_{axial}	1.18	Axial Chord (in)	c_{axial}	1.53	Axial Chord (in)
s	1.08	Spacing (in)	s	0.77	Spacing (in)
o	0.54	Throat Opening (in)	o	0.74	Throat Opening (in)

5.5. LPT Structural Analysis

Similar to HPT structural analysis, similar calculations are made for LPT. The only difference is LPT does not require extra cooling considerations.

The average annulus area (A) is 59.99 in² which is bigger than HPT's annulus area. Also this will be helpful with the stress since the bigger area it gets the smaller force applied per unit area. The rotational speed (ω) is 1802.3 rad/s for Low Pressure Turbine. Average Centrifugal stress (σ_{ave}) for LPT is found as 25.71 ksi which shows the relation of area and stress.

Table 5.10 : LPT Stage Turbine Blade Measurements

2nd Stage Turbine Blade Stresses					
Blade Widths Vane			Blade Widths Rotor		
W_{vane} (ft - in)	0.108	1.298	W_{rotor} (ft - in)	0.142	1.704
h_3 (ft - in)	0.108	1.293	h_{4R} (ft - in)	0.128	1.541
h_4 (ft - in)	0.128	1.541	h_{5R} (ft - in)	0.157	1.889
Stress Calculations					
$W_{\text{dr}}/W_{\text{vane}}$	0.5600		$W_{\text{dr}}/W_{\text{rotor}}$	0.5600	
$W_{\text{dr-rim}}$ (ft - in)	0.061	0.727	$W_{\text{dr-rim}}$ (ft - in)	0.080	0.954
h_r / r_r	0.05		h_r / r_r	0.05	
r_r (ft - in)	0.425	5.098	r_r (ft - in)	0.401	4.815
ρ_3 (lbm/ft ³)	0.085		ρ_4 (lbm/ft ³)	0.047	
λ (taper ratio)	0.70		λ (taper ratio)	0.70	
A_3 (ft ² - in ²)	0.339	48.762	A_4 (ft ² - in ²)	0.495	71.224
σ_c (psi)	28282.53		σ_c (psi)	23135.01	
A_{ave} (in ²)				59.99	
$\sigma_{c\text{-ave}}$ (psi)				25708.77	

Similar to HPT, Carbon Fiber Reinforced SiC CMC material is selected for LPT vanes and rotors. Cooling for this section is not necessary due to lower temperature of the stage. Since the temperature and stress values are lower on the LPT, creep life is expected to be more than HPT stage.

To conclude, all the calculations shows that CMC (ceramic matrix composite) is the well suited material for turbine blades. For the new engine case, Carbon Fiber Reinforced SiC CMC is selected for the vane and rotor blades due to their higher tensile strength, higher operational temperature limits, strong resistance for oxidization and stability to corrosion.

6. INLET DESIGN

RFP suggests a 2-ramp inlet, either axisymmetrical or 2-dimensional configuration which enables new engine works efficiently. New inlet is selected as a 2-dimensional which more suitable for new nacelle and cheaper to produce. On 2-ramp inlet design, 2 oblique shock waves and 1 normal shock wave at throat occur.

Since new engine will be used on T38 trainer aircraft, the inlet and its geometry should be simple, light and cheap to ensure the working conditions of the engine. Therefore, non-variable 2-ramp inlet without auxiliary air inlets is preferred. Besides, the latest improvement in T38 inlet [U10] shows that with bellmouth inlet prototype, static phase and all operation conditions are able to be met. Therefore, similar however better version of inlet is aimed.

Inlet face area is determined by maximum speed, where speed is 1.4 Mach at 40 kft. At this condition, obtaining the ramp angles that provide maximum pressure recovery is analysed. Corrected mass flow is taken as 50.5 lbm/s from performance analyses program. Moreover, existing nacelle envelope is preferred, which is less 18-inch fan diameter. So, inlet duct will be a transition duct to provide changing the shape form a rectangular to a circular geometry.

Oswatitsch [19] introduced a method on similar external compression ramp inlets. In order to reach out the maximum pressure recovery, oblique shocks should have same power, which is used in the inlet ramp angles design phase. Additionally, due to the boundary layer effect, it is suggested to add 4% safety margin into the area [4].

Table 6.1 : Ramp Angles & Inlet Output

External 2 Ramp Compression			
M_1		1.4	
1st Oblique Shock		2nd Oblique Shock	
θ_1	4.367	θ_2	3.759
β_1	51.71	β_2	62.179
M_2	1.24102102	M_3	1.072491669
P_{t1} / P_{t0}	0.9990	P_{t2} / P_{t1}	0.9990
Normal Shock			
M_4	0.9339	P_{t3} / P_{t2}	0.9996
ΔP_t		0.9975	

At flight speed 1.4 Mach, required inlet face area ratio is A/A^* is found as 1.115. With 4% safety margin, this area ratio is reached to 1.16. At the end, inlet area is found as 1.225 ft² (176.4 in²).

After the normal shock, air goes through the transition zone. Crosthwait [20] states that the length of transition zone is twice of the height of the throat. At last, diffuser takes air to the nose of the engine. Our diffuser geometry changes from rectangular cross section to circular one in order to meet engine.

Table 6.2 : Inlet Diffuser Duct Data

Diffuser Duct	
M_i	0.93
M_e	0.46
A_e / A_i	1.44
L / D	3.5
η_D	0.90
P_{te} / P_{ti}	0.98
Y / D	1.55

At the zero flight speed condition, inlet size must be checked. When the improvement on T-38 inlet is evaluated [U10], a need for bellmouth lip can be seen. On the net inlet design, we will try to implement this need.

Typical diffuser portion of supersonic inlet from Mattingly [4] is taken into consideration of our inlet.

While designing bellmouth lip section, analytical comparisons have been made. For 0.35 Mach throat number at zero flight inlet condition, 1.5 in thick bellmouth makes contribution of 96.86% pressure recovery. However, the required inlet area is not enough to ensure SLS operation. Therefore, 1.2 in long elliptical inlet lip design is chosen in order to reach out bigger suction strength on the intake face. Since this estimation needs to be experimentally measured and checked, it is fine to make these basic assumptions to reach out the required inlet area of 1.84 ft².

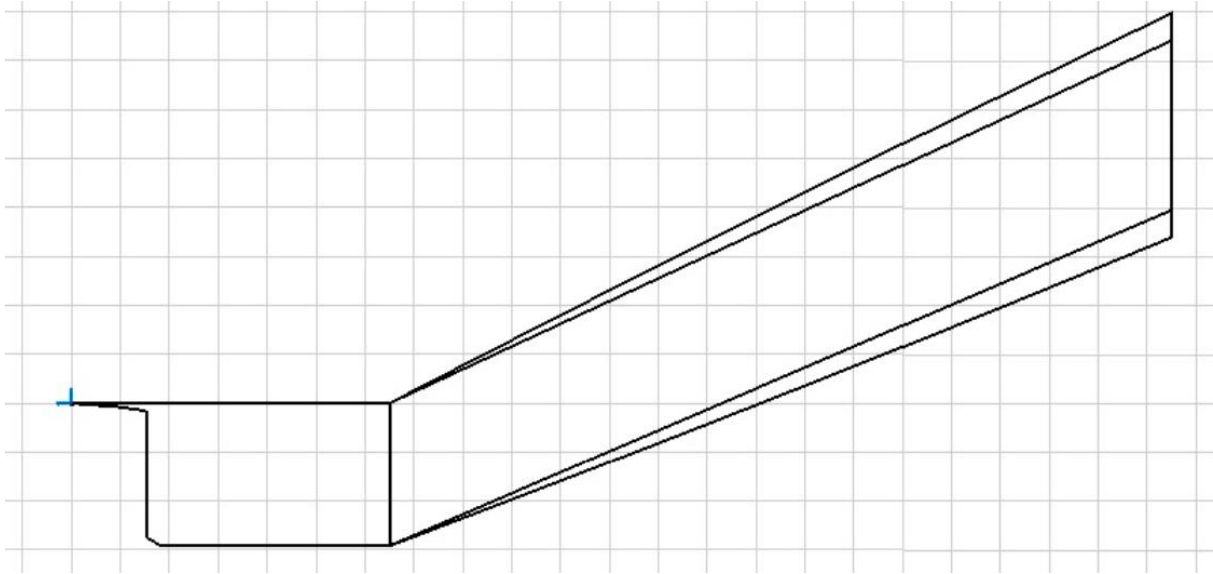


Figure 6.1 : Inlet Geometry

The inlet geometrical details are:

- Height: 9.21 in & Width: 18.42 in
- Transition duct length: 18.42 in
- Diffuser length: 63 in
- Lip elliptic length: 1.2 in

7. COMBUSTION SYSTEMS DESIGN

Combustion systems are designed with the help of Mattingly and Farokhi [4, 6].

7.1. Main Burner

Among the 3 burner types, annular combustion system which provides weight advantages and higher pressure recovery is selected for the new engine.

Design point for combustions systems is at SLS condition. On this condition, engine has the maximum dynamic pressure condition in the main burner area, which will have significant effect on the design.

Table 7.1 : Main Burner Stations & Dimensions

Stations Dimensions	Station 3.1	Station Burner	Station 4
R_{outer} (in)	5.582	6.271	6.298
R_{inner} (in)	5.218	5.009	5.702
R_{mean} (in)	5.400	5.640	6.000
H (in)	0.363	1.262	0.597

The combustion system operates with a better efficiency on slower velocities. From our HPC stages, the velocity coming to main burner is approximately 0.35 Mach, which is quite a high value. Therefore, the speed of air coming from HPC needs to be slowed down to minimize the pressure loss with a diffuser design.

The diffuser system is preferred as flat wall geometry with 2 splitters. Splitters provide a shorter and more efficient operations for such situations. The length of the diffuser is measured as 1.94 in, which its axial length is 1.92 in. Furthermore, with the adequate mix,

burner total pressure loss is calculated as 10.04 psi, around 80% of the allowable value of 12.29 psi, which is acceptable.

Table 7.2 : Air Partitions at $T_g = 1950\text{K}$ (3510°R) & $\epsilon_{pz} = 0.8$

Air Partitions	Total	Primary Zone	Secondary Zone	Transpiration Cooling	Dilution Zone
Air Flow (lbm/s)	22.727	9.943	4.261	3.636	4.886
Mass Fraction	1.000	0.438	0.188	0.160	0.215

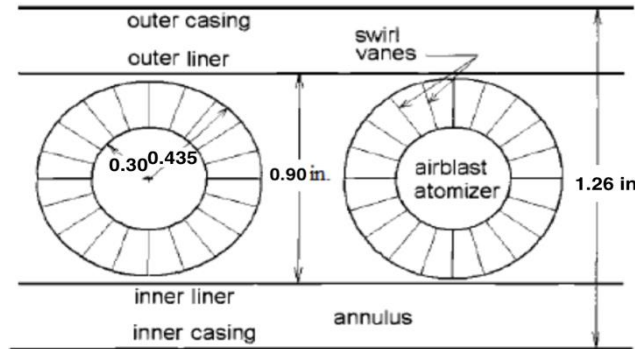


Figure 7.1 : Swirler Design & Layout

Swirler blades have been chosen as airfoil cross-sections with 0.64 drag coefficient and 40° blade angle. Also swirl number is found as 0.76, which is a good value between 0.60 and 1.00 limits. As last step of main burner, zones and geometry are measured as:

Table 7.3 : Main Burner Zones Geometry

Zones Geometry			
N_{primary}	28	L_{primary} (in)	0.659
$N_{\text{secondary}}$	260	$L_{\text{secondary}}$ (in)	1.740
N_{dilution}	168	L_{dilution} (in)	1.305

Table 7.4 : Main Burner Geometry

Burner Geometry	
Length (in)	3.704
Diameter (in)	1.262
Total Volume (ft ³)	0.096
Combustion Zone (ft ³)	0.074

7.2. After-Burner

Afterburner radius is considered as 9 in, (0.75ft) which is fan and diameter of the new engine. Both air from LPT (stage 5) and bypass duct (stage 16) enters afterburner section of the engine. Before the burner, mixer and its geometry calculations are made. In order to ensure the small dimensions on this section, mixer-diffuser design option is selected. The most important part is to ensure the velocity coherency of the both air streams which might otherwise create structural damages inside the engine.

Table 7.5 : Flow Areas before After-Burner Section

Dimensions	Station 5	Station 6	Station 13	Station 16	Station 6A	Station 7
r_{outer} (in)	6.945	7.260	9.000	8.700	9.000	9.000
r_{mean} (in)	6.000	5.125	8.400	7.980	6.300	4.500
r_{inner} (in)	5.055	2.990	7.800	7.260	3.600	0.000
A (in ²)	71.224	137.493	63.335	72.201	213.754	254.469
H (in)	1.889	4.270	1.200	1.440	5.400	9.000

On the 7th stage, the velocity of mixed stream is approximately 440ft/s, which corresponds to 0.257 Mach at ~650K temperature.

Mixer optimum area is measured from the Mattingly [4] and results are listed in Table 7.6 and Figure 7.2. Diffuser efficiency for new design is 96.4%, which is quite a good value.

Table 7.6 : Mixer & Diffuser Dimensions

Dimensions	Station 6A	Station M	Station 6.1
r_{outer} (in)	9.00	9.00	9.00
r_{mean} (in)	6.30	5.40	4.50
r_{inner} (in)	3.60	1.80	0.00
A (in ²)	213.75	244.29	254.47
H (in)	5.40	7.20	0.00



Figure 7.2 : Mixer & Diffuser Layout

Vee-Gutter angle for flameholders is selected as $2\theta = 30^\circ$. Besides, W/H value is chosen as 0.4, which corresponds to $D/H = 0.314$ values to minimize the pressure loss on afterburner.

As last, ring number is selected as 2 to decrease the length of afterburner tube. Afterburner geometry can be found in figure 7.3 below.

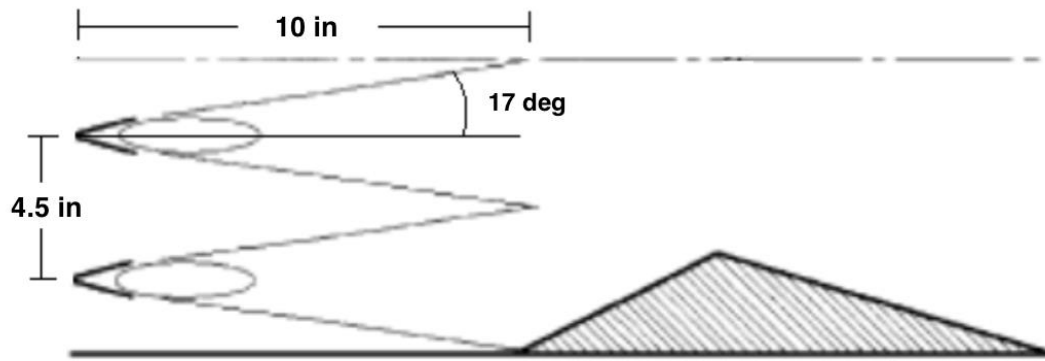


Figure 7.3 : Flameholders Layout

On the last step, few more important data for the burner and afterburner can be found in table 7.7.

Table 7.7 : Combustion Parameters

Combustion Parameters					
Burner		Design Guideline	After Burner		Design Guideline
Combustor Loading (kg/s atm ^{1.8} m ³)	0.5	Maximum 10	Combustor Loading (kg/s atm ^{1.8} m ³)	5.16	Maximum 100
Combustor Intensity (MW/atm m ³)	~ 30	Maximum 60	M_AB	0.267	Max. 0.3

8. NOZZLE DESIGN

Nozzles has a significant effect on specific fuel consumption and thrust by changing its operating conditions. Efficiency of engine is strongly dependent of nozzle which increases the velocity of the exhaust gas to have a higher kinetic energy for higher thrust.

In modern aircrafts, engine exhaust system provides efficient expansion of gasses to ambient pressure, low installation drag, low noise, low cooling requirements, light-weight system and low-cost manufacturability. These are also design goals to meet the requirements of RFP.

RFP requires an appropriate convergent-divergent noise-attenuating nozzle which enables efficient supercruise and current noise restrictions at take-off. Performance comparison of De Laval (convergent – divergent) nozzle versus convergent nozzle in Farokhi [6] proves that De Laval nozzle is more suitable for our new engine. From parametric cycle analysis, NPR range is between 2.4 - 4.8 which gains the thrust by at least 5% when compared to a convergent nozzle, which is another positive effect.

Due to afterburner operations of the new engine, a variable nozzle area is a must. 5th generation fighter aircrafts have also high maneuver property thanks to their ultimate powerful engines and thrust vectoring property. In order to simulate extreme turns and high maneuvers in the training simulations, a thrust vectoring ability of nozzle is desired. Additionally, thrust vectoring is able to increase the effectiveness of aircraft for certain activities and mission

segments. Furthermore, circular nozzle throat type is also chosen because of it is better pressure recovery than rectangular nozzle throat [4].

Even though it is desirable to reach perfect expansion with convergent – divergent nozzle, it is not possible to ensure this condition for all the flight conditions. Over-expansion and under-expansion conditions are not possible to be avoided. Therefore, it is better to consider these details in our nozzle design. Because of the higher pressure loss of over-expanded nozzle [21], a small margin is taken into design.

Variable nozzle area properties will be determined by the 2 most important flight conditions of the aircraft. The smallest area occurs when the minimum mass flow passes through nozzle, while the highest are happens on maximum pressure ratio. These 2 conditions are respectively obtained on cruise (dry) and maximum speed conditions (full wet). Because of our goal of increasing the maximum speed of new engine, we consider 1.4 Mach on our design.

Lastly, in order to reach out the best nozzle, design needs to be optimized considering dimension, performance and weight properties.

From the own developed performance analysis program and Mattingly source [4], we have obtained nozzle design input values in Table 8.1.

Table 8.1 : Nozzle Design Input Values

Nozzle Design Input	Flight Condition	
	Cruise at 35 kft	Max Mach on 40 kft
Mass Flow Rate (lbm/s)	20.21	28.44
Pressure Loss	0.988	0.988
Throat Mach Number	1.00	1.00
Flight Mach Number	0.85	1.4
T _{t8} (R)	971.64	3240
P _{t9} /P ₀	3.83	7.20
Exit Mach Number (real)	1.53	1.96
A ₉ / A ₈	1.20	1.71
Max Discharge Coefficient	0.94	0.98

Table 8.2 : Nozzle Design Output Values

Nozzle Design Output	Flight Condition	
	Cruise at 35 kft	Max Mach on 40 kft
Exit Mach Number (ideal)	1.54	1.97
Exit Mach Number (real)	1.53	1.96
Velocity Coefficient	0.995	0.9975
Primary Half Angle (degrees)	30.7	17.01
Secondary Half Angle (degrees)	3.4	14.38
Throat Radius (in)	5.34	7.11
Exit Radius (in)	5.85	9.30
Primary Nozzle Length (in)	6.17	
Secondary Nozzle Length (in)	8.54	
Total Nozzle Length (in)	14.71	

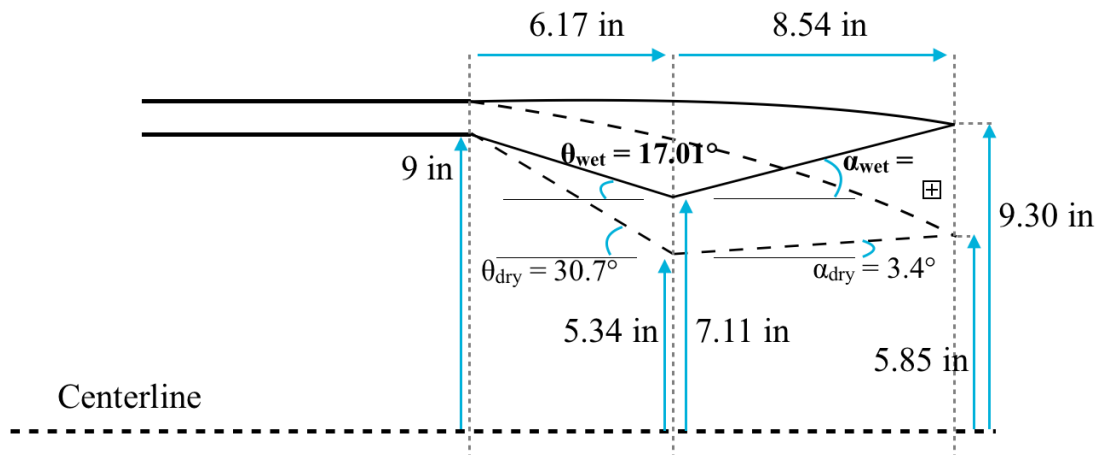


Figure 9.1 : New Convergent – Divergent Nozzle Geometry

9. CONCLUSION

Through this project, a better version of J85-5A engine is developed by forcing the design and technology limits. At the end, a comparison is made as following in table 9.1:

Table 9.1 : J85-5A & New Engine Comparison Summary

Properties	J85-GE-5A		BeEngine	
	DRY	WET	DRY	WET
Thrust (lbf)	2 680	3 850	2 750	4 600
TSFC (1/h)	1.03	2.20	0.66	1.76
Airflow (lbm/s)	44.1		50	
OPR	6.7		16	
ByPass Ratio	-		1.2	
Compressor Stages	9		2F, 0L, 6H	
Turbine Stages	2		1H, 1L	
Diameter (inc)	22		20 (18 by Fan)	
Lenth (inc)	108.1		80	
Weight (lbm)	584		425	

A summary of selected materials for each component is listed below in table 9.2:

Table 9.2 : New Engine Component vs. Material Summary

Components	Material
Fan / LPC	Ti-6Al-4V
HPC	Greek Ascoloy
Burner	SiC/SiC CMC
HPT	Carbon Reinforced SiC CMC
LPT	Carbon Reinforced SiC CMC
Nozzle	Ti-MMC (Metal Matrix Composite)

With the new developed engine, a better performance and efficiencies are achieved for new T-38 aircraft.

For the future actions, due to the very small geometry of the engine, further analyses are recommended to obtain real working operations of the new engine. Especially the boundary layer and CFD analyses of the entire engine would be very useful. Since this project is prepared for AIAA competition, these analyses are not included inside this project report.

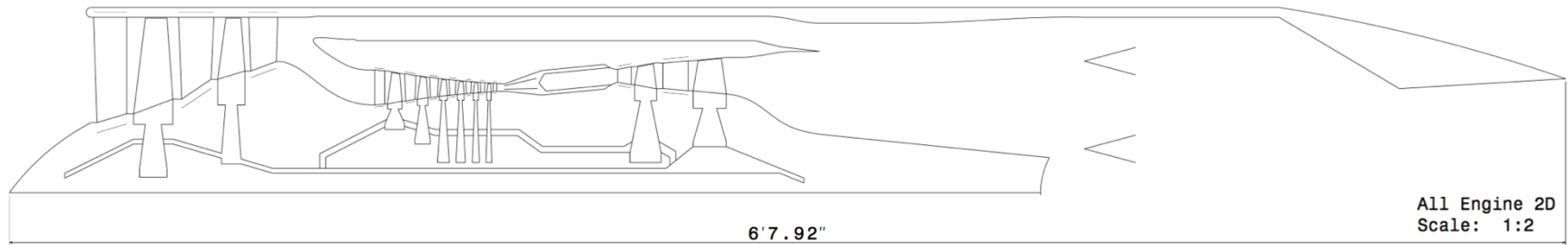
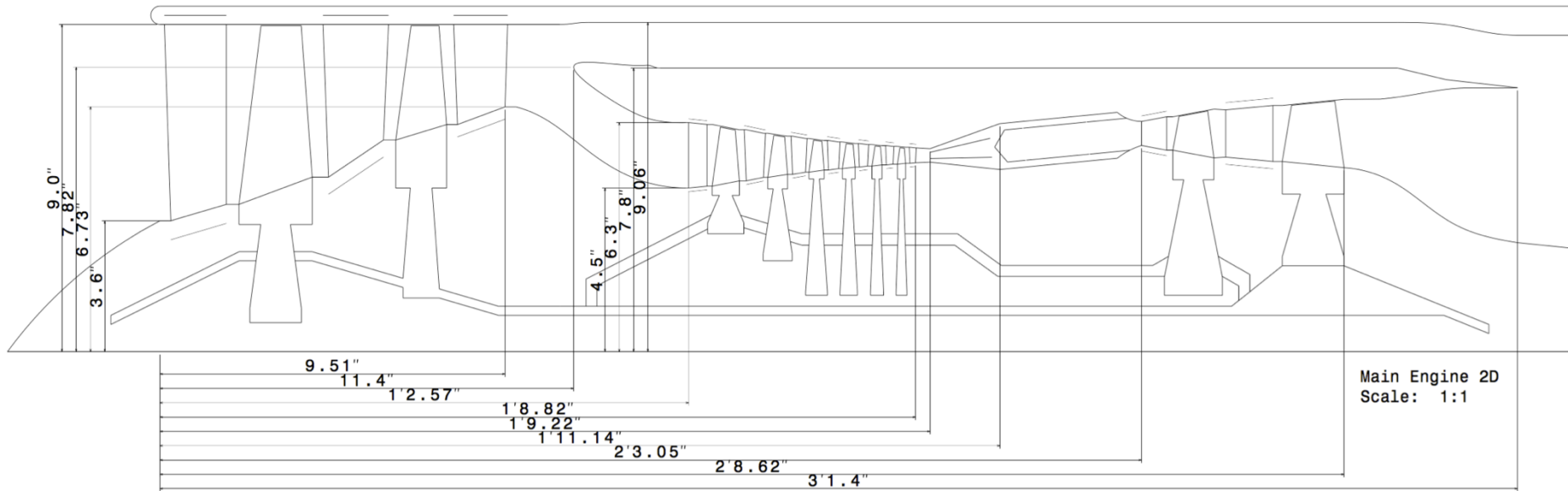


Figure 9.1 : BeEngine 2D Preliminary Technical Draftings

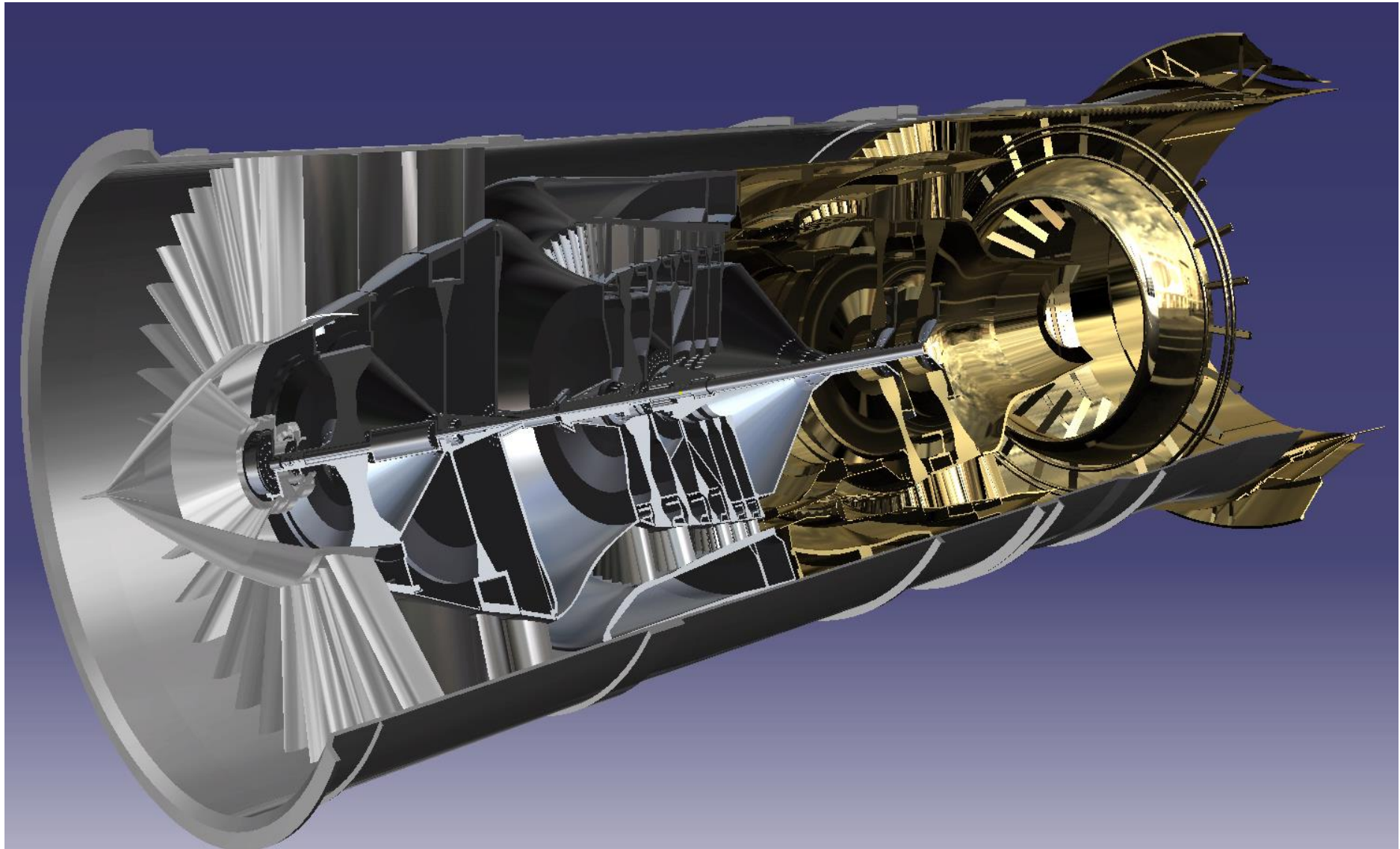


Figure 9.2 : BeEngine 3D Technical Drawing (Nozzle is on wet contition)

REFERENCES:

- [1] Lockheed Martin. (2007), **F-35 Defining the Future**.
- [2] Roux, E. (2007). **Turbofan and Turbojet Engines: Database Handbook**. ISBN: 978-2-9529380-1-3.
- [3] Younossi, O., Arena M. V., Moore R. M., Lorell M., Mason J., & Graser J. C. (2002). **Military Jet Engine Acquisition – Technology Basics and Cost-Estimating Methodology**. United States Air Force, RAND.
- [4] Mattingly, J. D., Heiser, W.H. & Pratt, D. T. (2002). **Aircraft Engine Design**. 2nd Ed. AIAA.
- [5] NASA (2003). **T-38 Flight Manual**.
- [6] Farokhi, S. (2014). **Aircraft Propulsion**. 2nd Ed. Wiley.
- [7] Greitzer E. M. & Slater H. N. (March 31, 2010). **Design Methodologies for Aerodynamics, Structures, Weight, and Thermodynamic Cycles – Final Report**. MIT - Aurora Flight Sciences and Pratt&Whitney Team.
- [8] Moffitt, T. P., Szanca, E. M., Whitney, W. J. & Behning, F. P. (1980). **Design and Cold-Air Test of Single-Stage Uncooled Turbine With High Work Output**. NASA.
- [9] Dixon, S. L., & Hall, C. A. (2010). **Fluid Mechanics and Thermodynamics of Turbomachinery**. 6th. Ed.
- [10] “GE Tests CMCs for Future Engine”, Aviation Week & Space Technology, July 30, 2012.
- [11] Dixon, S. L., & Hall, C. A. (2010). **Fluid Mechanics and Thermodynamics of Turbomachinery**. 6th. Ed.
- [12] GE Aviation. (2015). **GE Successfully Tests World’s First Rotating Ceramic Matrix Composite Material for Next-Gen Combat Engine**. Retrieved from http://www.geaviation.com/press/military/military_20150210.html, date retrieved 10.01.2016.
- [13] GE Global Research. **Ceramic Matrix Composites Improve Engine Efficiency**. GE Global Research. <http://www.geglobalresearch.com/innovation/ceramic-matrix-composites-improve-engine-efficiency>, date retrieved 10.01.2016.
- [14] Raether, F. (2003). **Ceramic Matrix Composites – an Alternative for Challenging Construction Tasks**
- [15] Bansal, N.P. & Lamon, J. (2015). **Ceramic Matrix Composites - Materials, Modeling and Technology**
- [16] Halbig, M. C., Jaskowiak M. H., Kiser J. D. & Zhu D. (2013). **Evaluation of Ceramic Matrix Composite Technology for Aircraft Turbine Engine Applications**. NASA.
- [17] Hess, W. G. (1979). **Laminated Turbine Vane Design and Fabrication**. NASA.
- [18] Jakus & Nair, (1995). **Temperature Mechanical Behavior of Ceramic Composites**.x
- [19] Goldsmith, E. L. & Seddon, J. (1993). **Practical Intake Aerodynamic Design**. AIAA.
- [20] Crosthwait, E. L., Kennon, I. G., & Roland, H. L. (1967). **Preliminary Design Methodology for Air-Induction Systems**. Technical Report: SEG-TR-67-1. Wright-Patterson Air Force Base, Ohio.
- [21] Gamble E., Terrel D. & DeFrancesco R, (2004). **Nozzle Selection and Design Criteria**. AIAA.
- [U1] Url-2, AIAA, **2015-2016 Team Engine Design Competition** <<http://www.aiaa.org/RFP2015-2016EngineDesignComp/>>, date retrieved 04.01.2016.
- [U2] Url-2, NASA, **T-38s Soar as Spaceflight Trainers** <http://www.nasa.gov/mission_pages/shuttle/flyout/t38flyout.html>, date retrieved 04.01.2016.
- [U3] Url-3, Motor Sich, **AI-222-25F** <<http://www.motorsich.com/eng/products/aircraft/tde/ai-222-25f/>>, date retrieved 10.01.2016.
- [U4] Url-4, Lockheed Martin, **F119 Product Card** <http://www.pw.utc.com/Content/F119_Engine/pdf/b-2-3_me_f119_product_card.pdf>, date retrieved 10.01.2016.
- [U5] Url-5, Lockheed Martin, **F135 Specs Charts** <http://www.pw.utc.com/Content/F135_Engine/pdf/B-2-4_F135_SpecsChart.pdf>, date retrieved 10.01.2016.
- [U6] Url-6, Lockheed Martin, **F135 Product Card** <http://www.pw.utc.com/Content/F135_Engine/pdf/b-2-4_me_f135_ctol.pdf>, date retrieved 10.01.2016.
- [U7] Url-7, SATURN, **117S** <<http://www.npo-saturn.ru/?sat=64>>, date retrieved 10.01.2016.
- [U8] Url-8, Japan Ministry of Defence, **XF-5: 16 Research demonstration engine** <<http://www.mod.go.jp/j/approach/hyouka/seisaku/results/21/jigo/>>, date retrieved 10.01.2016.
- [U9] Url-9, United Engine Corporation, **AL-31F** <http://www.uk-odk.ru/eng/products/military_aviation/al31f/>, date retrieved 10.01.2016.
- [U10] Url-10, **Improved Inlets for T-38 Airplane** <<http://www.techbriefs.com/component/content/article/ntb/tech-briefs/mechanics-and-machinery/2580>>, date retrieved 10.01.2016.

APPENDIX A - Performance Analysis – Iterative Solution Method Scheme

$\tau_{tH} \approx \text{constant}$, $\pi_{tH} \approx \text{constant}$ & $\tau_{tL} \approx \text{constant}$, $\pi_{tL} \approx \text{constant}$

$$C_1 \approx \text{constant} = \frac{\tau_r \tau_f}{\tau_\lambda} (\tau_{cH} - 1)$$

$$C_2 \approx \text{constant} = (1 + a)(\tau_f - 1) \frac{\tau_r}{\tau_\lambda}$$

$$C_3 \approx \text{constant} = a \pi_{cH} \sqrt{\frac{\tau_r \tau_f}{\tau_\lambda}}$$

$$C_2 = \left(\frac{\tau_r}{\tau_\lambda} + \frac{C_3}{(\tau_{cH})^{\frac{\gamma_{e_{cH}}}{\gamma-1}}} \sqrt{\frac{\tau_r}{\tau_\lambda \left(\frac{C_1 \tau_\lambda}{\tau_r (\tau_{cH} - 1)} \right)}} \right) \left(\frac{C_1 \tau_\lambda}{\tau_r (\tau_{cH} - 1)} - 1 \right)$$

$$\dot{m}_{c2-offD} = \dot{m}_{c2-D} \left(\frac{(1+a)_{offD}}{(1+a)_D} \right) \left(\frac{\pi_{c-offD}}{\pi_{c-D}} \right) \sqrt{\frac{\left(\frac{\tau_r}{\tau_\lambda} \right)_{offD}}{\left(\frac{\tau_r}{\tau_\lambda} \right)_D}}$$

